Solar Cells

Sung Hyun Jo

Ken Loh

EECS 598 Nanoelectronics Week 10 Presentation

November 1, 2005

Contents

- *Part1*
  - *Basic Operation*
  - *Key Parameters*
  - *Efficiency Limits & Losses*
- *Part2*
  - *Trend of Solar Cells Tech.*
  - *Design Rule*
- *Part3*
  - *Dye-Sensitized Solar Cells*
  - *Nanowire Dye-Sensitized Solar Cells*

Part 1

- *Basic Principles*
- *Key Parameters*
- *Efficiency Limits*
- *Efficiency Losses*

Solar Energy

- *Originates with the thermonuclear fusion reactions occurring in the sun.*
- *Represents the entire electromagnetic radiation (visible light, infrared, ultraviolet, x-rays, and radio waves).*

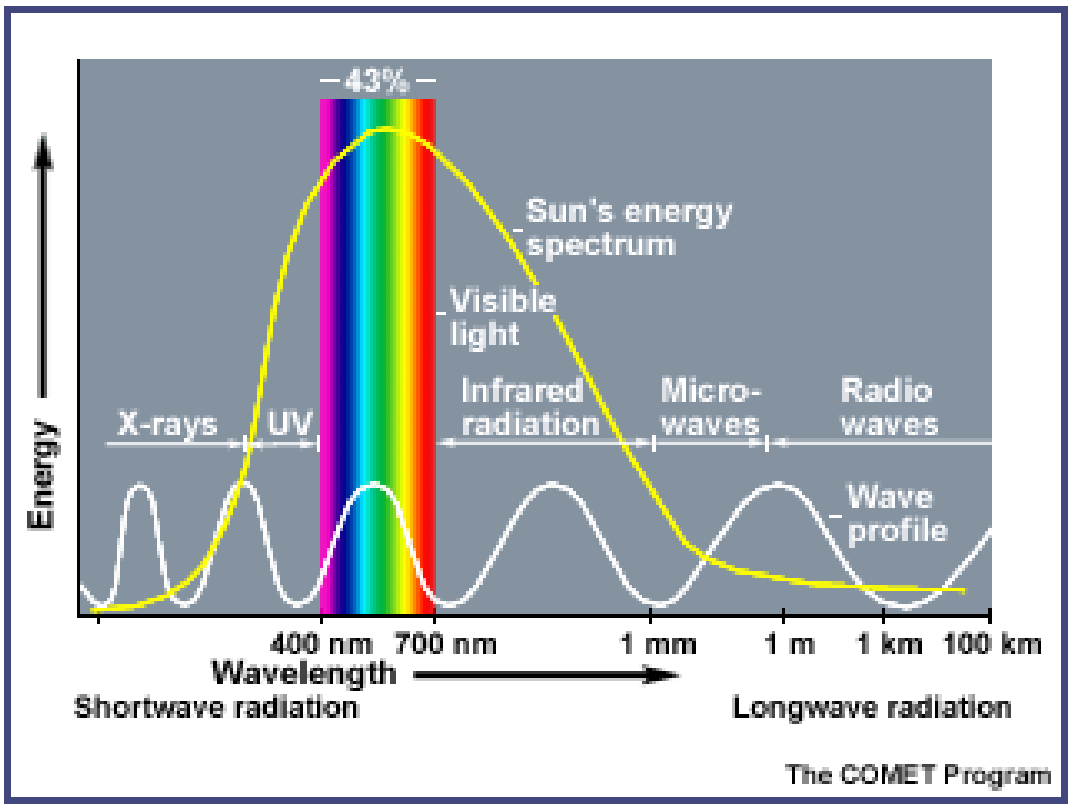

Conversion of Solar energy to Electricity

- **Solar Thermal Electricity**
  - General idea is to collect the light from many reflectors spread over a large area at one central point to achieve high temperature.
  - E.g. the 10-MW solar power plant in Barstow, CA.
    - 1900 heliostats, each 20 ft by 20 ft, a central 295 ft tower

Direct Conversion into Electricity

- Photovoltaic effect
  - ***Using a PN junction, directly convert photons into electrons and holes, and then separate them***

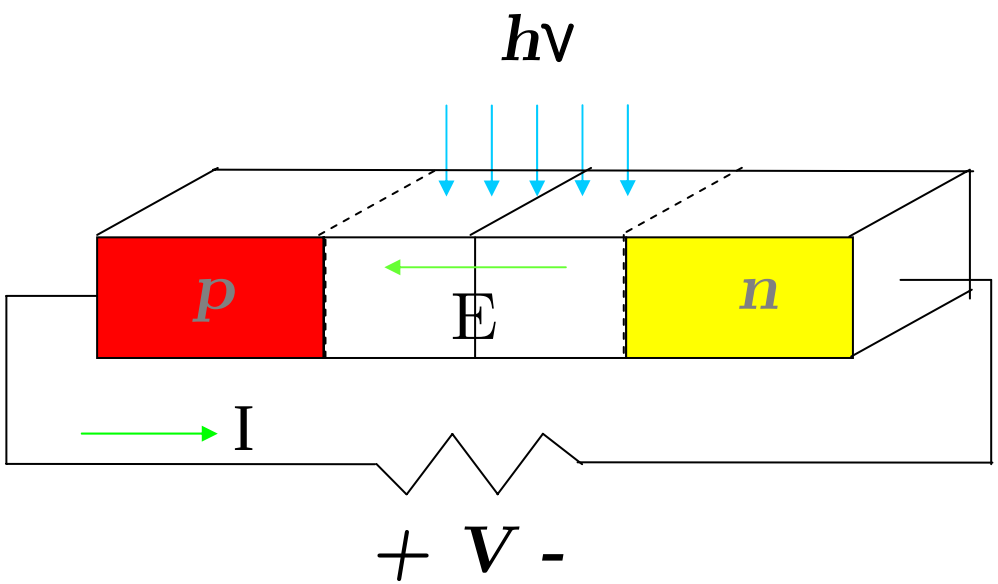

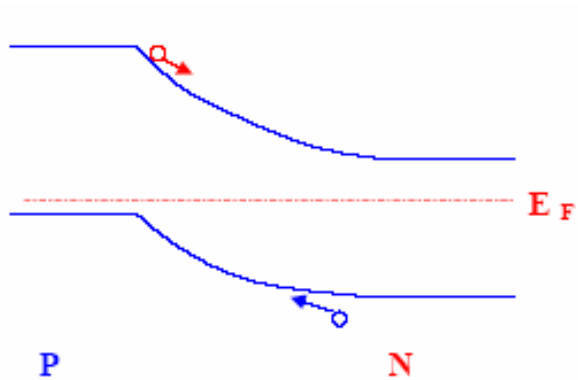

Type of Solar cells

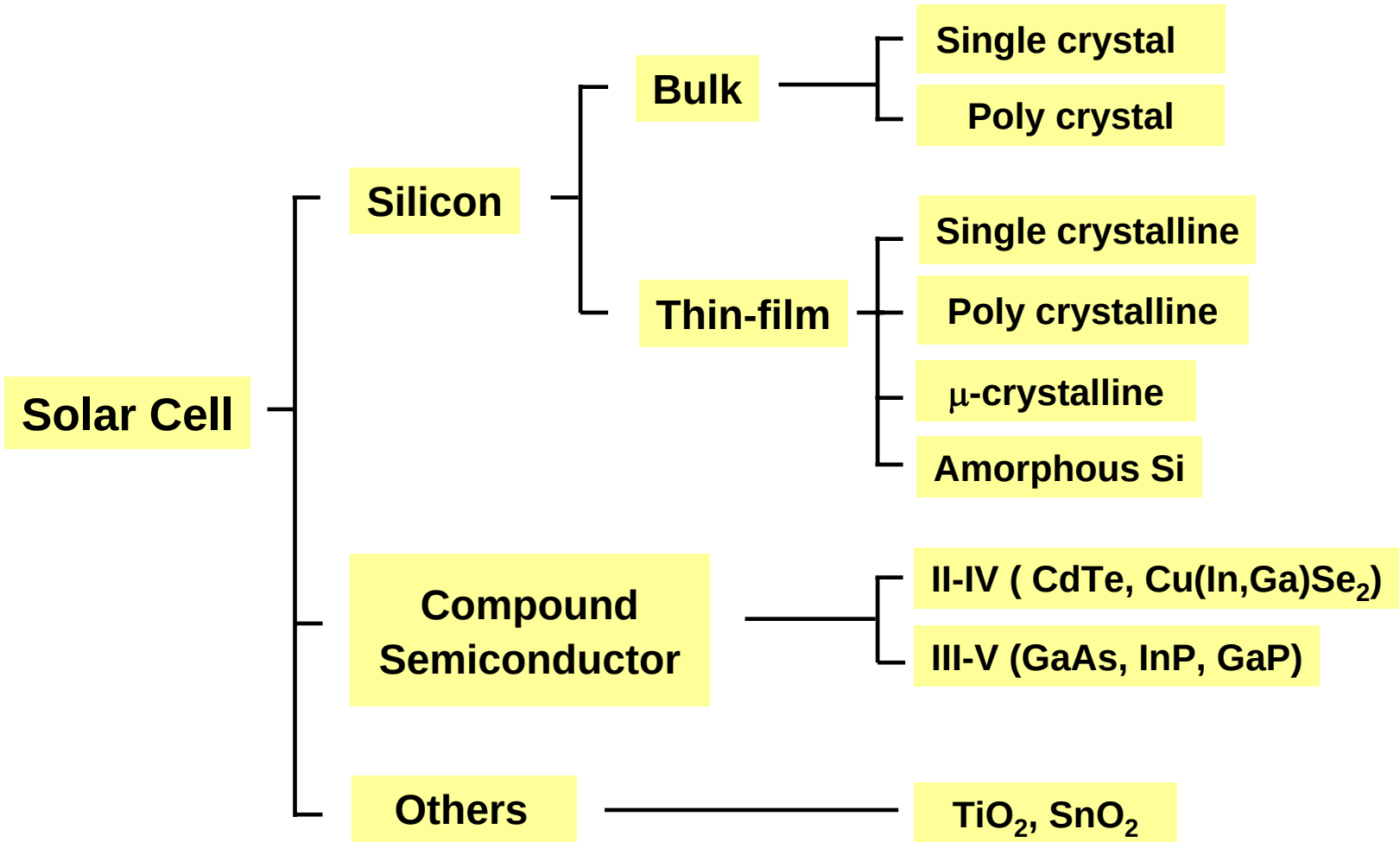

Electron-hole Pairs Generation

- When illuminated, excess electron-hole pairs are generated by light.
- Generated electrons flow from the p-type region to n-type.

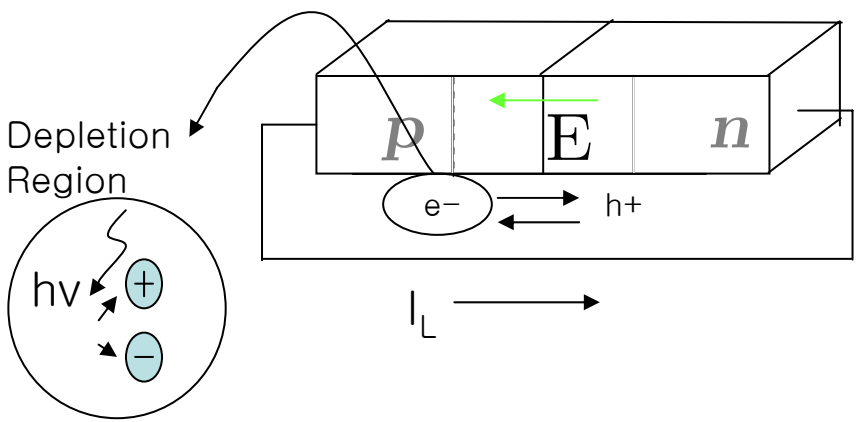

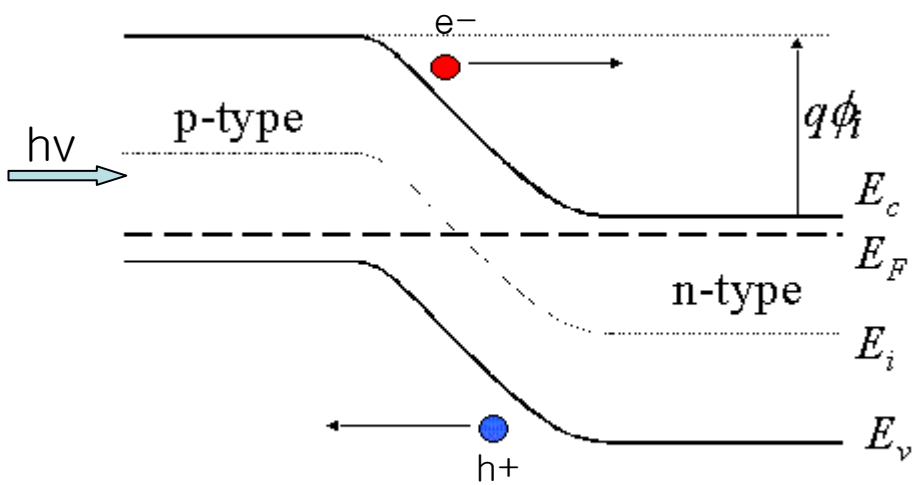

ILLUMINATED CHARACTERISTIC

- **Currents when illuminated**

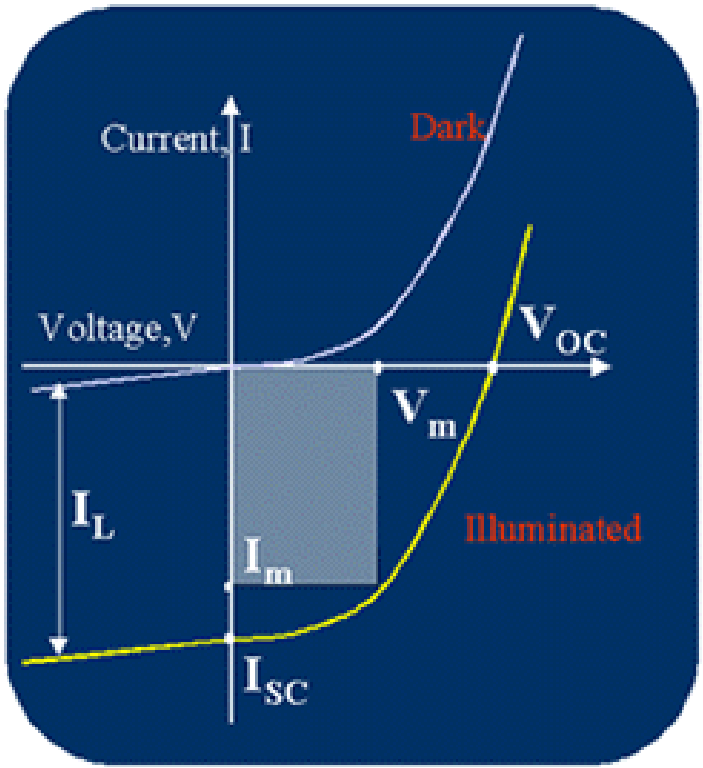

$$I_{dark} = I_0(e^{qV/kT} - 1)$$

$$I = I_0(e^{qV/kT} - 1) - I_L$$

$$I_L = qAG(L_e + W + L_h)$$

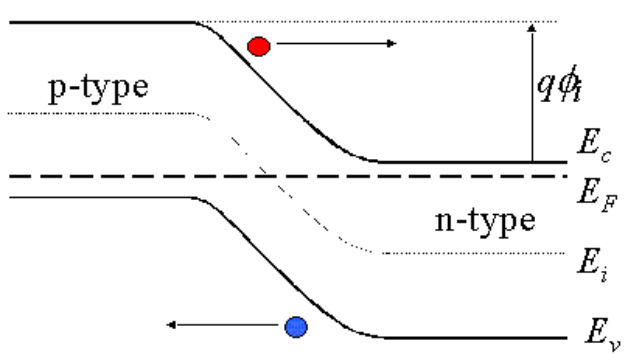

Key Parameters

- **Three parameters**
  - I_{sc} : Short-circuit current
  - V_{oc} : Open-circuit voltage

$$V_{oc} = \frac{kT}{q}\ln\left(\frac{I_L}{I_o}+1\right) \qquad \left(\because 0 = I_0(e^{qV_{oc}/kT}-1) - I_L\right)$$

  - FF (Fill Factor) : About max power, reasonably efficiency has a value of FF in the range 0.7 to 0.85

$$FF \triangleq \frac{V_m I_m}{V_{oc} I_{sc}}$$

  - Energy-conversion efficiency

$$\eta = \frac{V_m I_m}{P_{in}} = \frac{V_{oc} I_{sc} FF}{P_{in}}$$

(P_{in} : total power of the incident light)

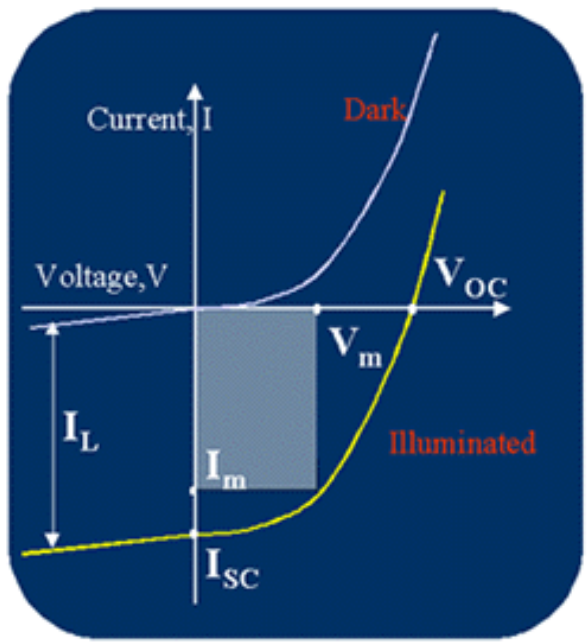

Efficiency Limits

$$\eta = \frac{I_{sc} V_{oc} \times FF}{P_{in}} \times 100\%$$

- **Short-Circuit Current Limit**
- **Open-Circuit Voltage Limit**
- **Fill-Factor Limit**

Short-Circuit Current Limit

Limit Maximum Jsc ⟵ **Material Bandgap [E(eV) =1.24/λ(um)]**
Photon Flux

$$J_{sc} = q \times \int_0^{\infty} Photon\_Flux(\lambda) d\lambda$$

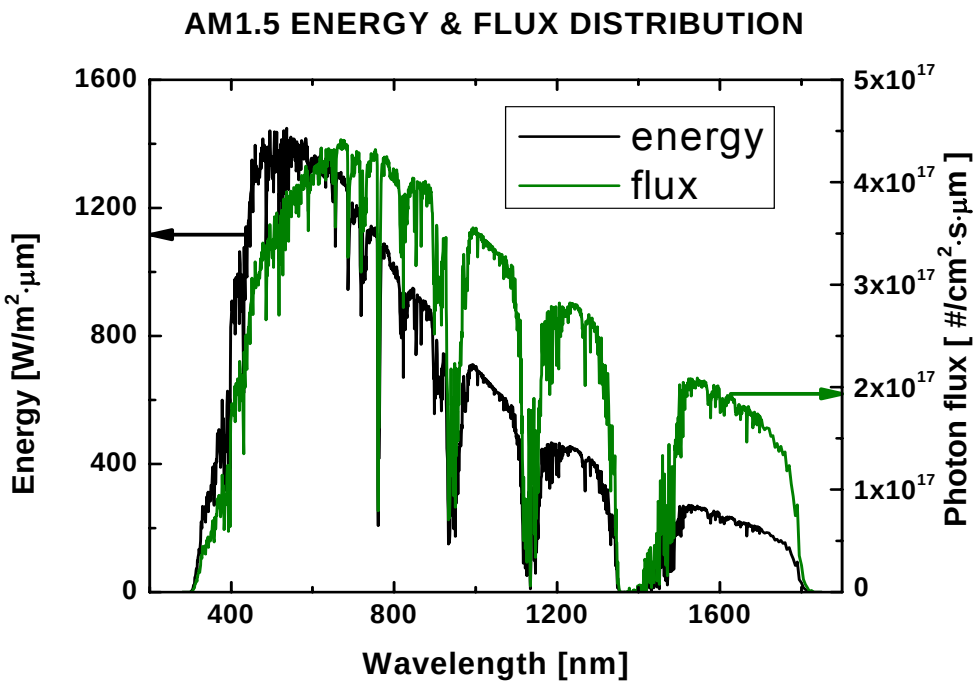

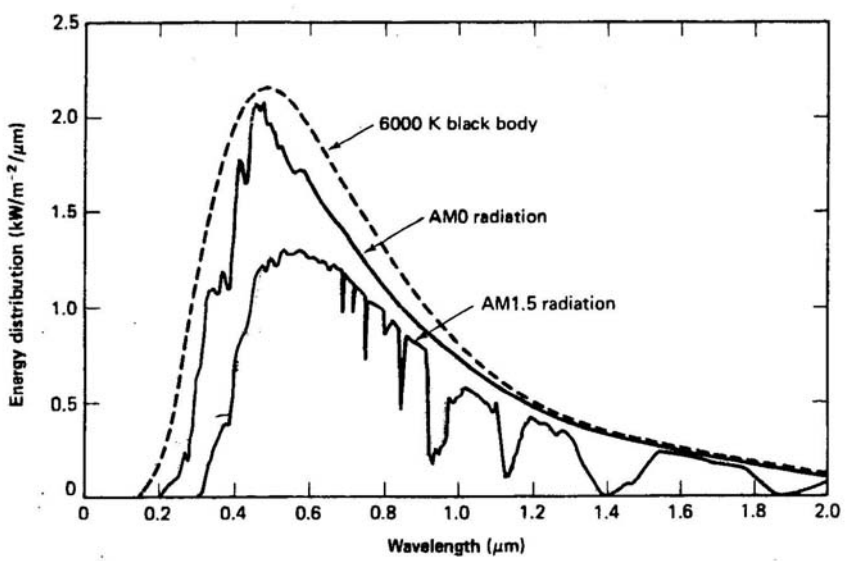

Calculated Results of Jsc

- ***Assume***:

  UNITY QUANTUM EFFICIENCY $(E_{PH} >= E_G)$

  ZERO QUANTUM EFFICIENCY $(E_{PH} < E_G)$

$E_g \downarrow \dashrightarrow I_{sc} \uparrow$

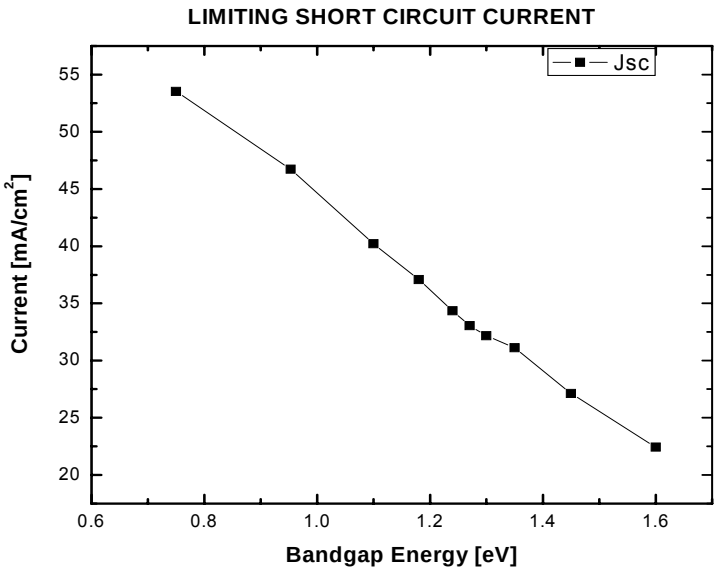

Material	Bandgap[eV]	Wavelength[㎛]	Jsc [mA/cm^2]
Ge	0.67	1.850	56.96
InGaAs	0.75	1.653	53.53
InGaAsP	1.10	1.120	40.22
Si	1.12	1.107	39.84
InP	1.35	0.918	31.12
GaAs	1.4	0.885	29.23

Open-Circuit Voltage Limit

Maximum Voc ⟵ **Short-Circuit Current**
Diode Saturation Current

$$V_{oc} = \frac{kT}{q}\ln\left(\frac{J_L}{J_0}+1\right)$$ ⟵

$$J = J_0\left[\exp\left(qV/kT\right)-1\right]-J_L$$

$$J_0 \propto \exp\left(-\frac{E_G}{kT}\right)$$

$$J_L = q\times\int_0^{\infty} Photon\_Flux(\lambda)\,d\lambda$$

$E_g \uparrow$ ⇢ $V_{oc} \uparrow$ $I_{sc} \downarrow$

Calculated Results of Voc & Eff.

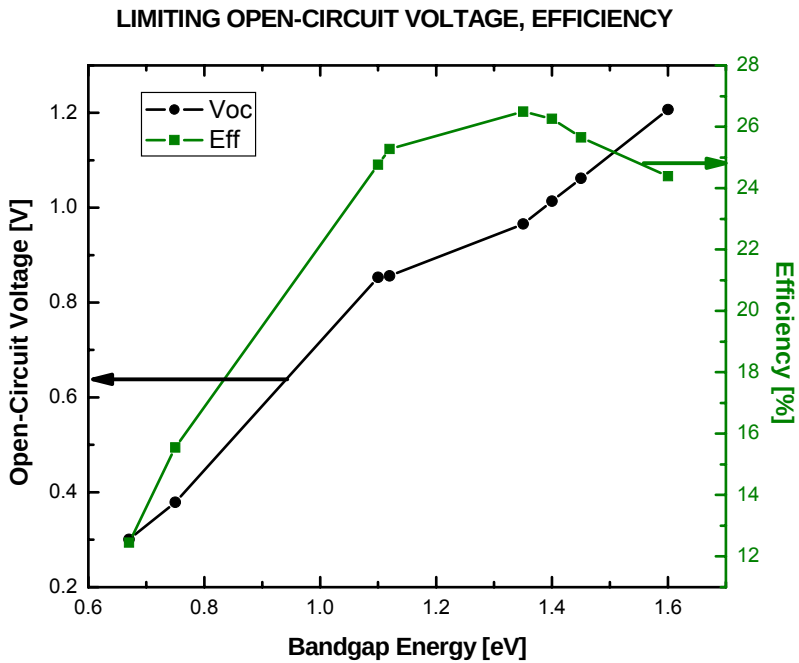

Optimum Bandgap
1.2~1.5 eV

Material	Bandgap [eV]	Voc[V]	Max. Eff [%]
Ge	0.67	0.3004	12.45
InGaAs	0.75	0.3789	15.55
InGaAsP	1.10	0.8531	24.76
Si	1.12	0.856	25.28
InP	1.35	0.9654	26.49
GaAs	1.4	1.0137	26.26

Efficiency Losses

- Fundamental limit
- Short-Circuit Current Losses
- Open-Circuit Voltage Losses
- Fill-Factor Losses

Why the efficiency is low ?

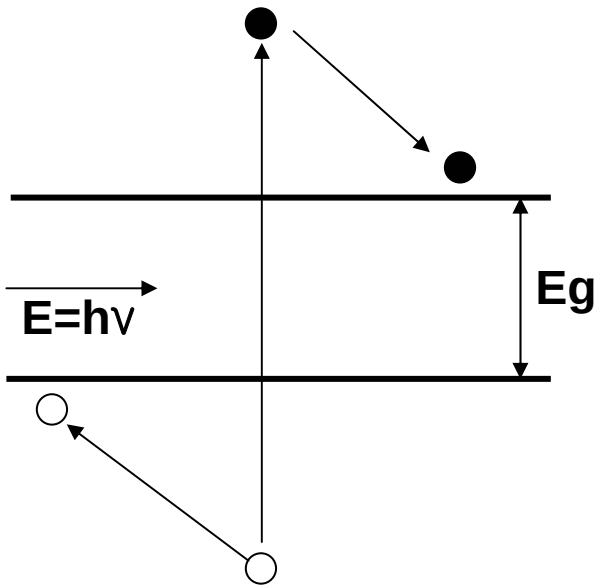

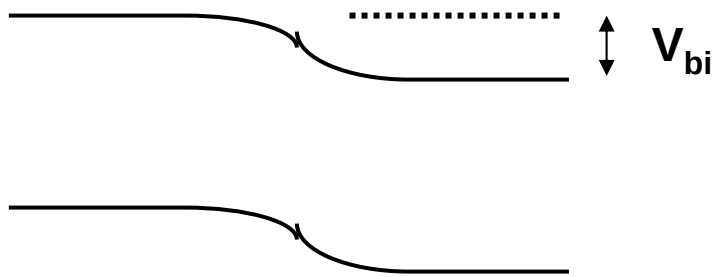

Loss : E(hν) - Eg

Voc < V_{bi} < Eg/q

Short-Circuit Current Losses

- Three types of losses

1. Reflection of Incident light at surface (~30%)
2. Hided Area due to Metal Grid Contact (5~15%)
3. Thickness of the Cell

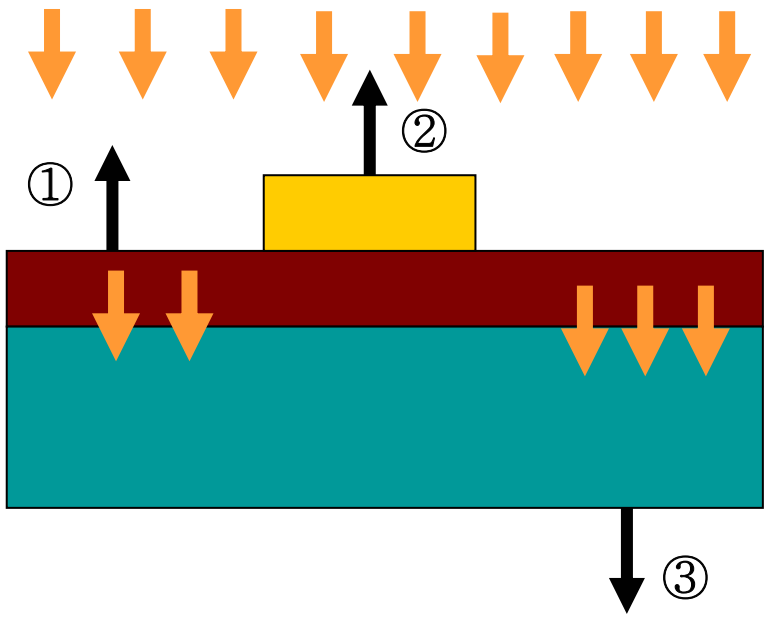

Index of refraction : $\hat{n}_c = \hat{n} - i\hat{k}$

K : extinction coefficient

$$R = \frac{(\hat{n}-1)^2 + \hat{k}^2}{(\hat{n}+1)^2 + \hat{k}^2}$$ (Normal incidence)

Experimental Results : AR Coating

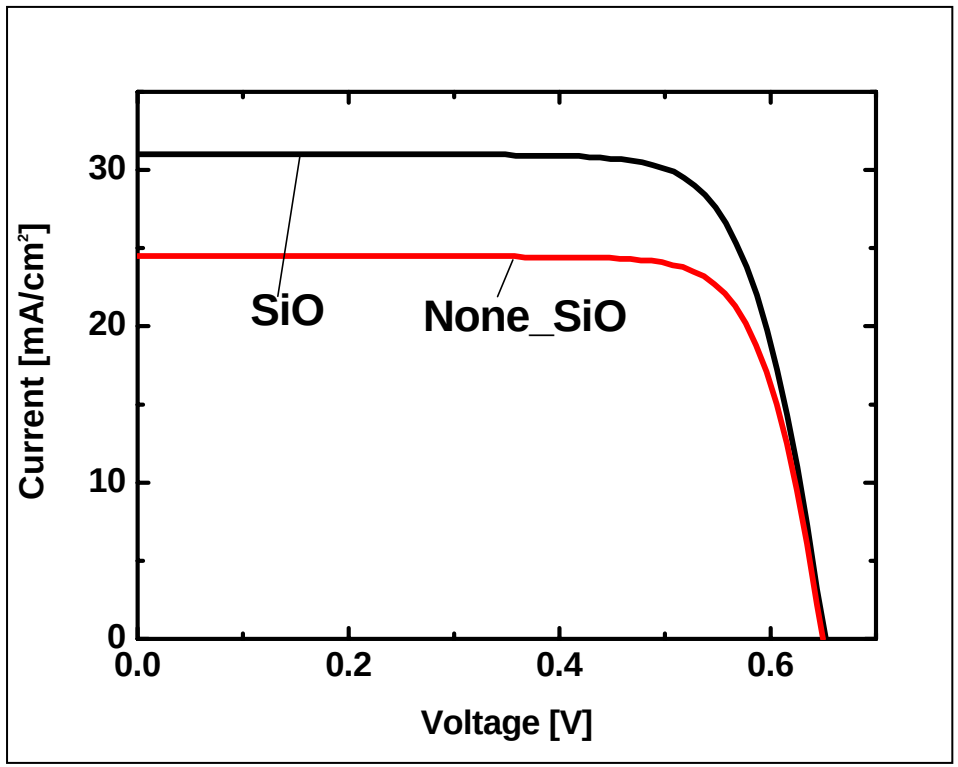

Open-Circuit Voltage Losses

- **Why the measured V_{oc} is lower than the limit of the V_{oc} ?**

  Fundamental Process : Recombination in Depletion Region

- **The Ideal Diode Equation**

$$J = J_0(e^{qV/kT} - 1)$$

- **Including Depletion-Region Recombination**

$$J = J_0(e^{qV/kT} - 1) + J_w(e^{qV/2kT} - 1)$$

Open-Circuit Voltage Losses

- **The Diode Equation**

$$J = J_0^{'}(e^{qV/nkT} - 1)$$

- **Ideal Open-Circuit Voltage**

$$V_{oc} = \frac{kT}{q}\ln(\frac{J_L}{J_0} + 1)$$

- **Measured Open-Circuit Voltage (n>1)**

$$V_{oc} = \frac{kT}{nq}\ln(\frac{J_L}{J_0^{'}} + 1)$$

Fill-Factor Losses

Recombination in Depletion Region → **Reduce Fill-Factor**

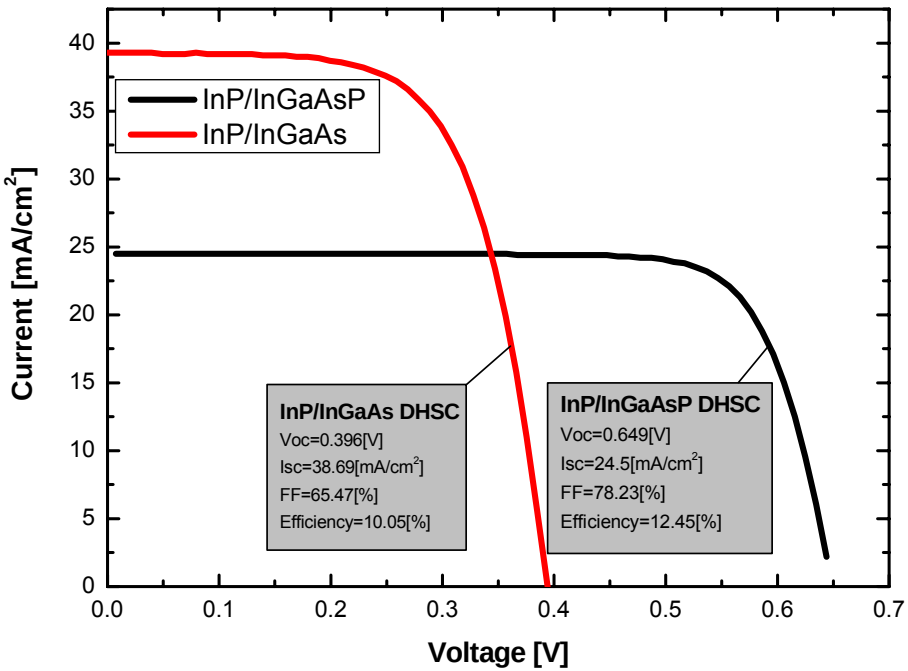

Fill-Factor Losses

- **Effect of Series and Shunt Resistant**

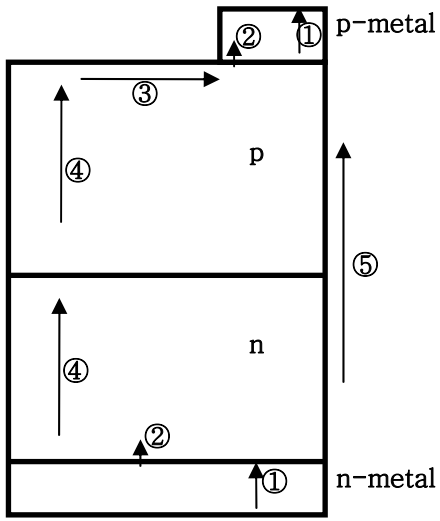

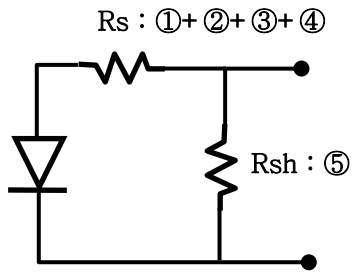

$$R_{CH} = \frac{V_{OC}}{I_{SC}}$$

$$r_s = \frac{R_S}{R_{CH}}$$

$$r_{sh} = \frac{R_{SH}}{R_{CH}}$$

$$FF = FF_0(1 - \alpha r_s)$$

Effect of Temperature

Operating Temperature of Solar Cells : Depends on place & time

I_{sc} & V_{oc}

Short-Circuit Current

$$J_{sc} = q \times \int_0^{\infty} Photon\_Flux(\lambda) d\lambda$$

$$E_{gT} = E_{go} - \frac{\xi T^2}{T + \theta_D} \qquad \xi \approx 5 \times 10^{-4} [eV / K] \qquad \theta \approx 200K$$

T ↑

- E_g → Slightly decreases
- J_{sc} → Slightly Increases
- V_{oc} → Slightly decreases

Part1 Summary

- **Basic Principle**
- **Efficiency Limits**

: Upper Limit → 26~29%(band gaps 1.2~1.5 eV)

- **Temperature Effect**

: Increasing temperature → Decreasing Open-Circuit Voltage

- **Efficiency Losses**

Part 2

- *Cost is one of the most important metrics*
  - *Trend of Solar Cell Tech.*
  - *Design Rule*

The Trend of Solar Cell Tech.

“ Improved Silicon Cell Technology ”

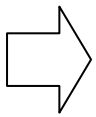

$ / Cell ↓

- ***Cost Down*** **: low cost substrate, processes**
  - *poly-crystalline silicon substrate*
  - *ribbon growth silicon substrate*
  - *diffusion by a spin on dopant (spray) process*
  - *metallization by screen printing*
  - *anti-reflection coating by spray process*
- ***Higher Efficiency***
  - *anti-reflection coating*
  - *texturing (light trapping)*
  - *multi-junction cells*
  - *back surface field*
  - *etc.*

Cost Analysis of Solar Cells

Cost Analysis of Solar Cells

ITEMS	1	2
Pure Si	38	38
Ingot Formation	115	35
Sawing	77	77
Wafer Cost	***230***	***150***
Cell Fabrication	80	80
Total Components	310	230
Yield	0.95	0.9
Cell Cost	***390***	***310***
Module Cost (Euro/m^2)	***476***	***406***
Efficiency	**0.14**	**0.12**

(" Handbook of Photovoltaic Science and Engineering", 2003)

Tandem Cell Structure

- **Connect in series several solar cells that have different band gap in the order $E_{g1} > E_{g2} > E_{g3}$.**
- **Each band gap must be selected to ensure same current flow.**

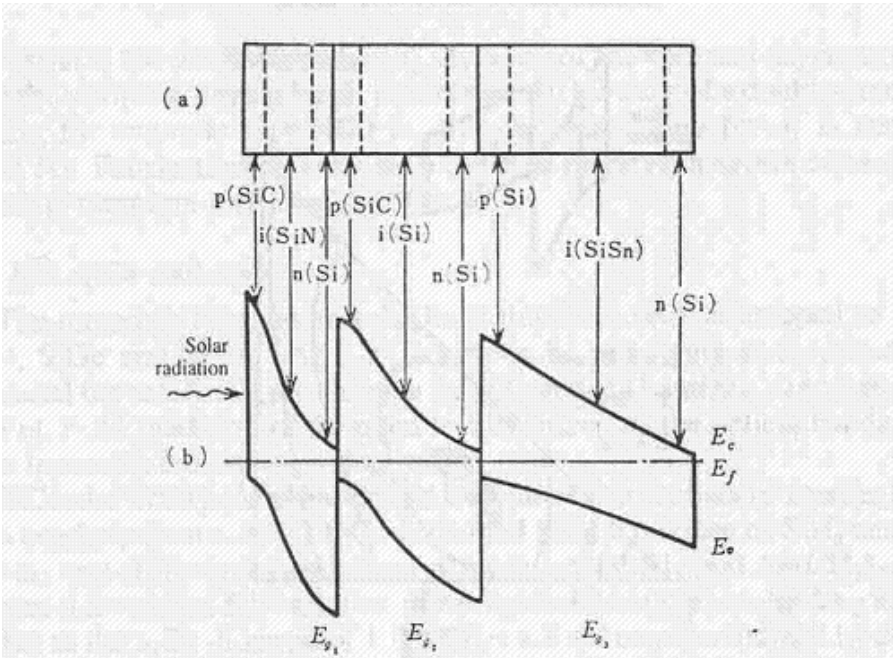

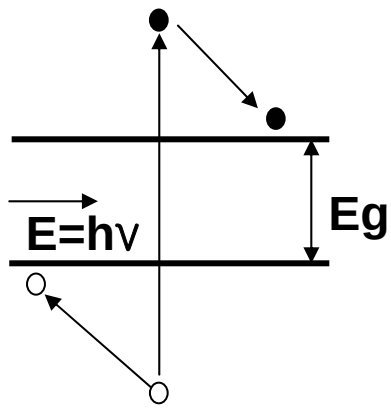

Loss : E(hν) - Eg

Tandem Cell Structure

Two Series Tandem Cell

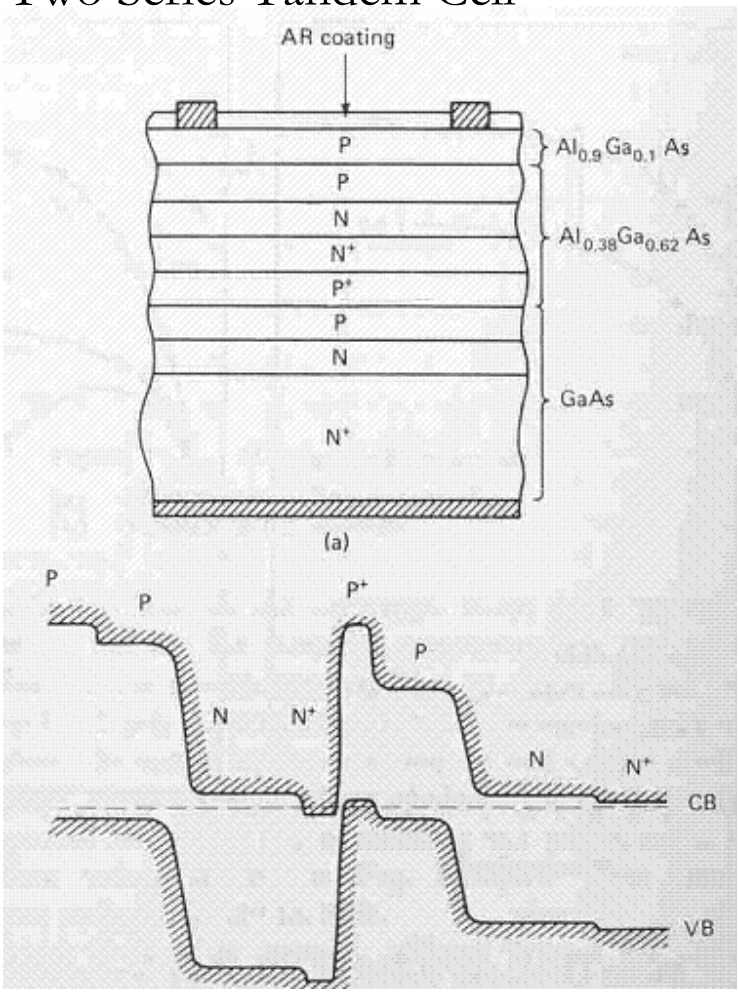

AlGaAs → ← GaAs

- **Top layer**
  - Window layer for underlying cell
- **Two heavily doped layer**
  - Back surface field
  - Tunneling process
  - Optical window for GaAs

Tandem Cell Structure

- **Theoretical conversion efficiency of two-layer tandem cell**

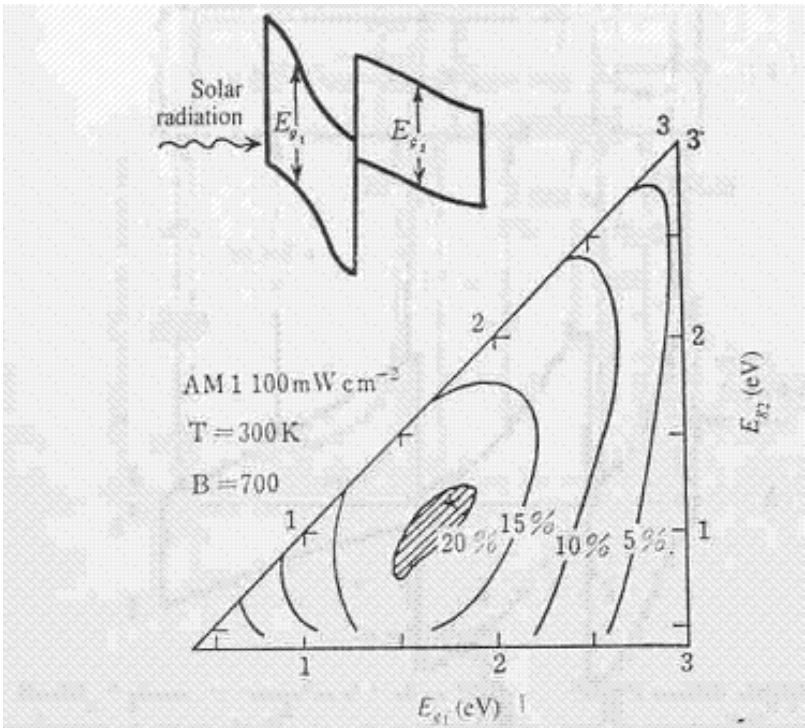

Maximum conversion efficiency (21%) when E_{g1}=1.75 eV & E_{g2}=1.15 eV

Tandem Cell Structure

- **The optimal set of bandgaps for tandem structures in unconcentrated sun**

n	η (%)	E_{g1} (eV)	E_{g2} (eV)	E_{g3} (eV)	E_{g4} (eV)
1	30	1·3	—	—	—
2	42	1·9	1·0	—	—
3	49	2·3	1·4	0·8	—
4	53	2·6	1·8	1·2	0·8

- **The optimal set of bandgaps for tandem structures in concentrated ratio 45900:1**

n	η (%)	E_{g1} (eV)	E_{g2} (eV)	E_{g3} (eV)	E_{g4} (eV)
1	40	1·1	—	—	—
2	55	1·7	0·8	—	—
3	63	2·1	1·2	0·6	—
4	68	2·5	1·6	1·0	0·5

Alloy Tech.

Alloy of InN & GaN ($In_xGa_{1-x}N$)

Bandgap changes 0.7~3.4 eV continuosly.

(InN:0.7 eV, GaN:3.4 eV)

Alloy of InN & AlN ($In_xAl_{1-x}N$)

Bandgap changes 0.7~6.2 eV continuosly.

(InN:0.7 eV, AlN:6.2 eV)

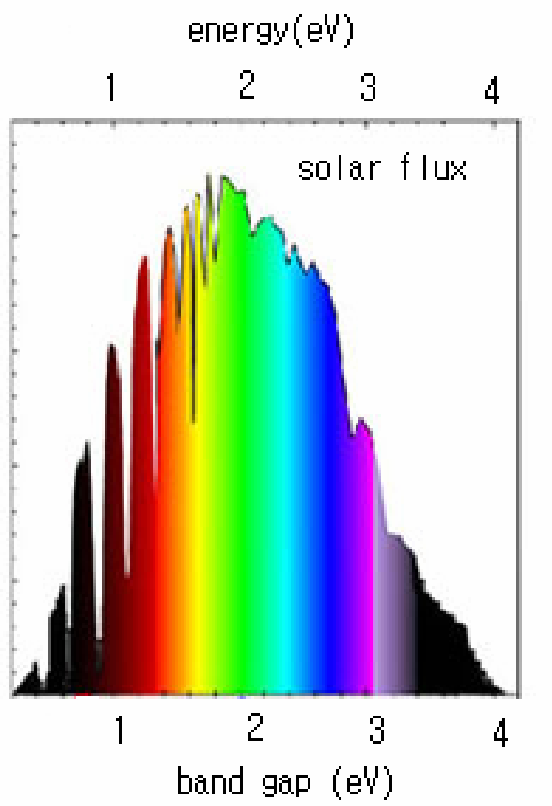

Design Rule

- **In PN Junction Solar Cell**
  - **Optimization**
    - **Junction depth and position**
    - **Doping concentration**

Collection Probability

- *The probability that the photo-generated carriers contribute to the actual current.*
  - *The function of distance in the cell*
  - *Important parameter*

Collection Probability

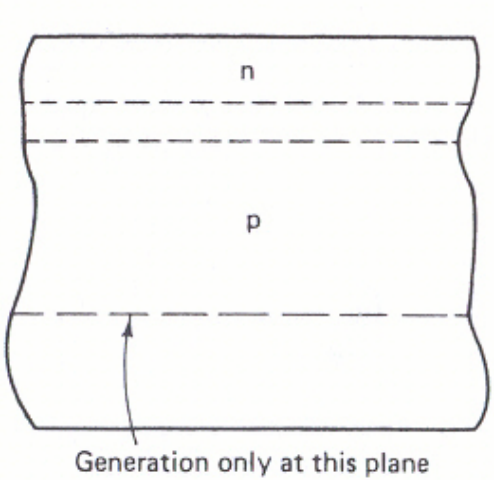

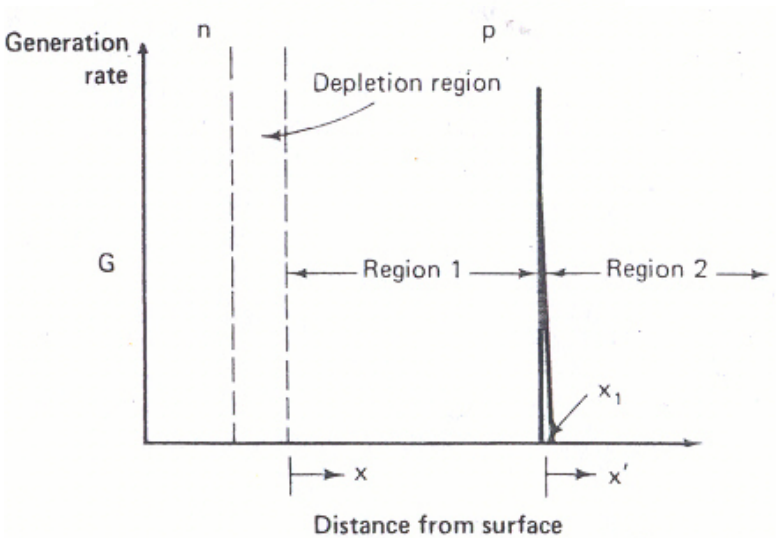

$$\frac{d^2\Delta n}{dx^2} = \frac{\Delta n}{L_e^2}$$

In region I ($0 < x < x_1$)

$$\Delta n = Ae^{x/L_e} + Be^{-x/L_e}$$

$$= A(e^{x/L_e} - e^{-x/L_e})$$

$$= 2A\sinh(\frac{x}{L_e})$$

In region II ($0 (= x_1) < x'$)

$$\Delta n = De^{-x'/L_e}$$

$$= 2A\sinh(\frac{x_1}{L_e})\sinh(-\frac{x'}{L_e})$$

Collection Probability

- Collection Probability : f_c

$$J_e = qD_e \frac{dn}{dx} = \frac{2qD_e A}{L_e} \cosh\left(\frac{x}{L_e}\right)$$

$$J_{DIS} = J_{e-} - J_{e+} = \frac{2qD_e A}{L_e} e^{x_1/L_e}$$

$$J_{SC} = J_e\big|_{x=0} = \frac{2qD_e A}{L_e}$$

$$f_C = \frac{J_{SC}}{J_{DIS}} \propto e^{-x_1/L_e}$$

Cells with PN junction near the surface have good performance

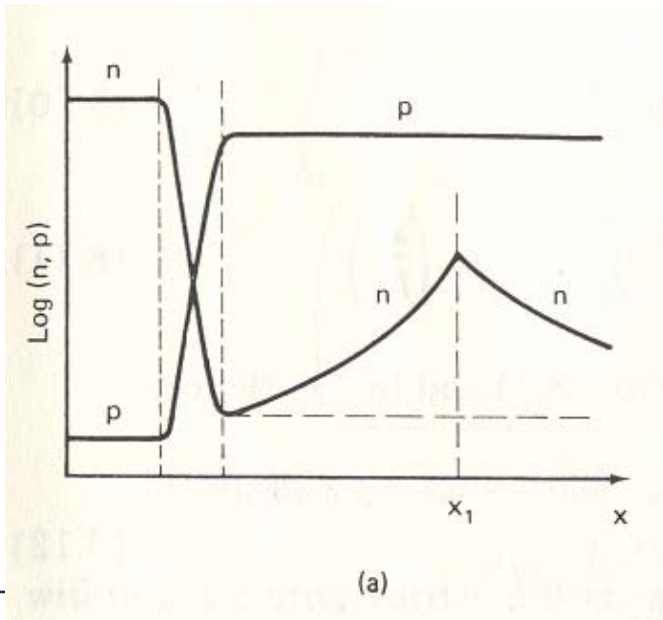

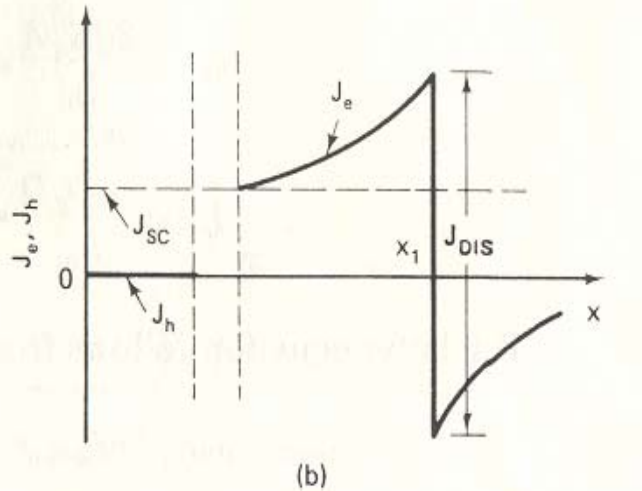

Collection Probability

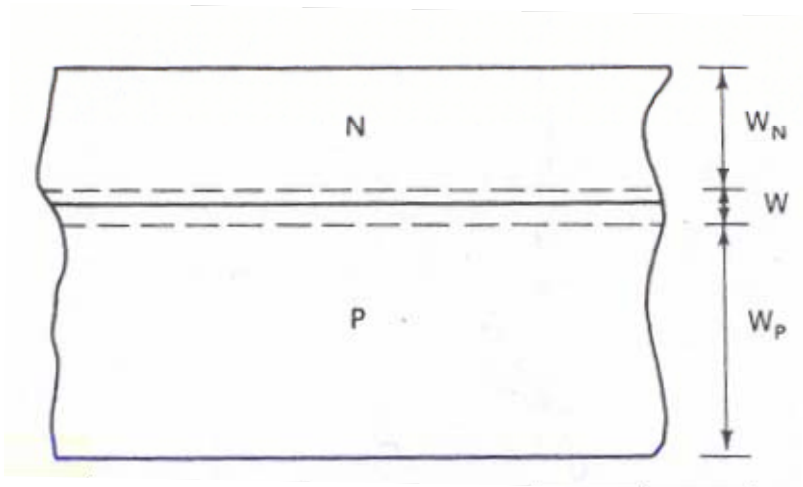

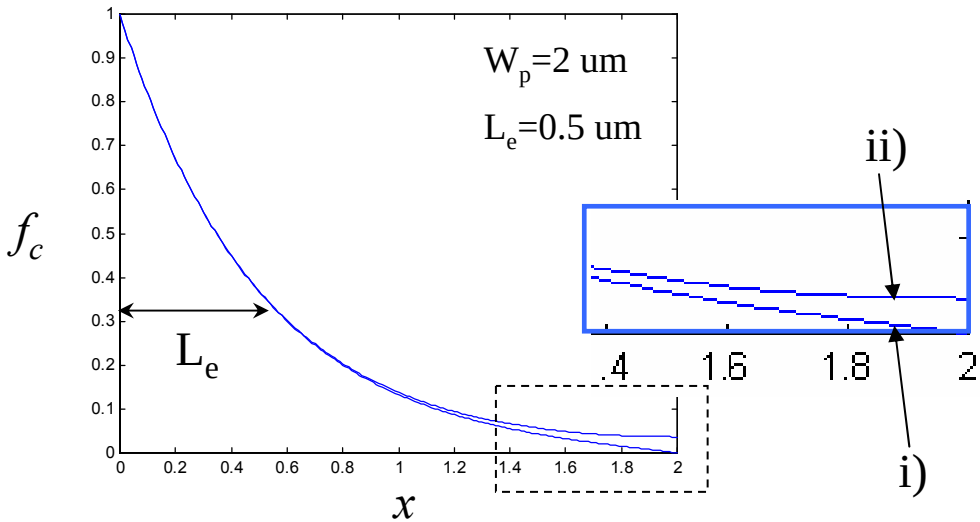

i) At X=W_p with high recombination

$$f_C = \frac{\sinh[(W_P - x)/L_e]}{\sinh(W_P/L_e)}$$

ii) At X=W_p with low recombination

$$f_C = \frac{\cosh[(W_P - x)/L_e]}{\cosh(W_P/L_e)}$$

Cells with lower recombination rate at back side show better performance

Back Surface Field

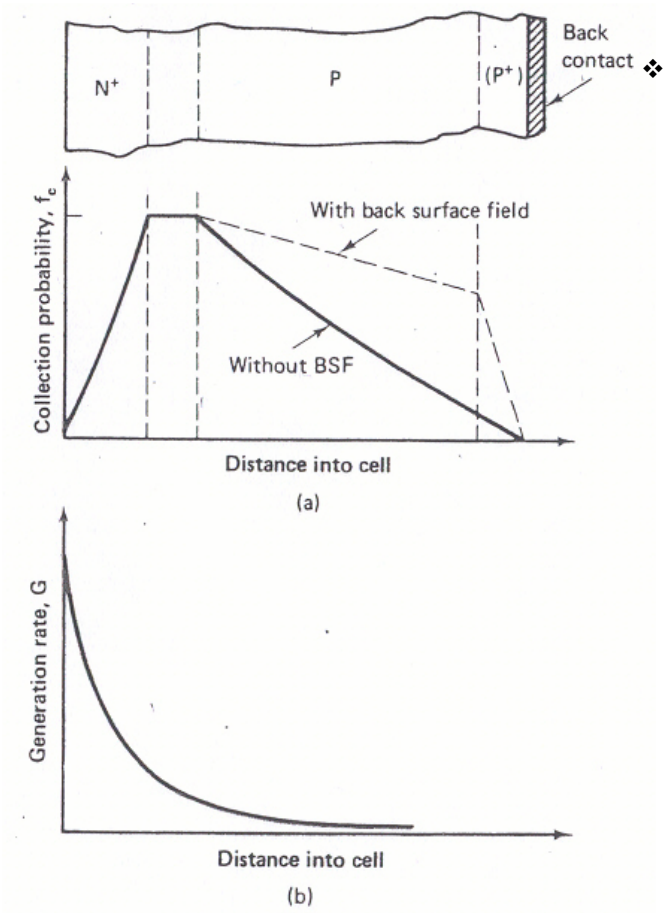

- The recombination at the back surface is usually very high (due to large contact area)
  - Reduce the recombination rate by highly doped region at back side

Part 2 Summary

- *For High Efficiency*
  - *Anti-reflection Coating*
  - *Textured Surface*
  - *PN junction near the surface*
  - *Low recombination rate at back side*
- *Low Cost Solar Cell Tech.*
  - *Crystalline into poly or amorphous material*
  - *Etc.*
- *Other possible approaches?*
  - *Dye-sensitized solar cells*

Nanowire Dye-Sensitized Solar Cells

Sung Hyun Jo

Ph.D. Student, Dept. of Electrical Engineering & Computer Science

Ken Loh

Ph.D. Student, Dept. of Civil & Environmental Engineering

EECS 598 Nanoelectronics Week 10 Presentation
Ann Arbor, MI

November 15, 2005

Research Motivation

- **Dye-sensitized cells (DSCs) promising devices for inexpensive, large-scale solar energy conversion**
  - Currently the most efficient and stable of excitonic photocells

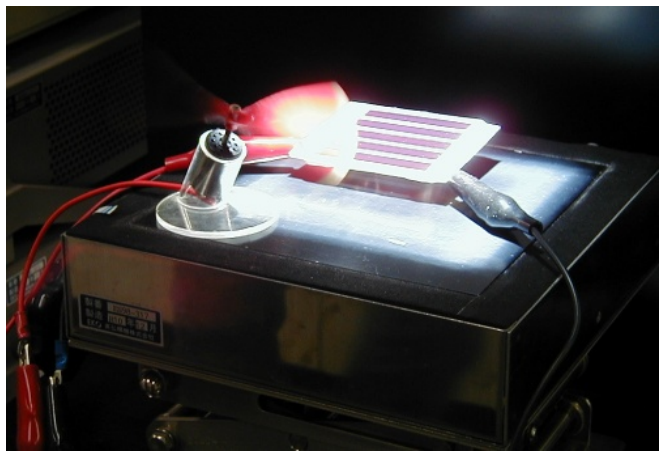

Left: Prototype dye-sensitized solar cell from the Solar Light Energy Conversion Group, Hideki Sugihara

- **Introduce a new version of the dye-sensitized cell**
  - Traditional nanoparticle film replaced with dense array of oriented, crystalline ZnO nanowires
  - Nanowire anode features a surface area up to one-fifth as large as a nanoparticle cell
  - Direct electrical pathways provided by the nanowires ensure the rapid collection of carriers generated throughout the device

Dye-Sensitized Solar Cells (DSCs)

- **Anodes typically constructed using thick films (~10 μm)**
  - TiO_2, SnO_2, or ZnO nanoparticles
  - Deposited as a paste and sintered to produce electrical continuity

- **Advantage**
  - Nanoparticle film provides large internal surface area
    - Characterized by roughness factor
      - Total film area per unit substrate area
    - For the anchoring of sufficient chromophore (usually ruthenium-based dye) to yield high light absorption in the 400 – 800 nm region
  - Maximum voltage corresponds to the difference between the redox potential of the mediator and the Fermi level of the semiconductor

- **Disadvantage**
  - Higher cost

Dye-Sensitized Solar Cells

- **Principle of operation**

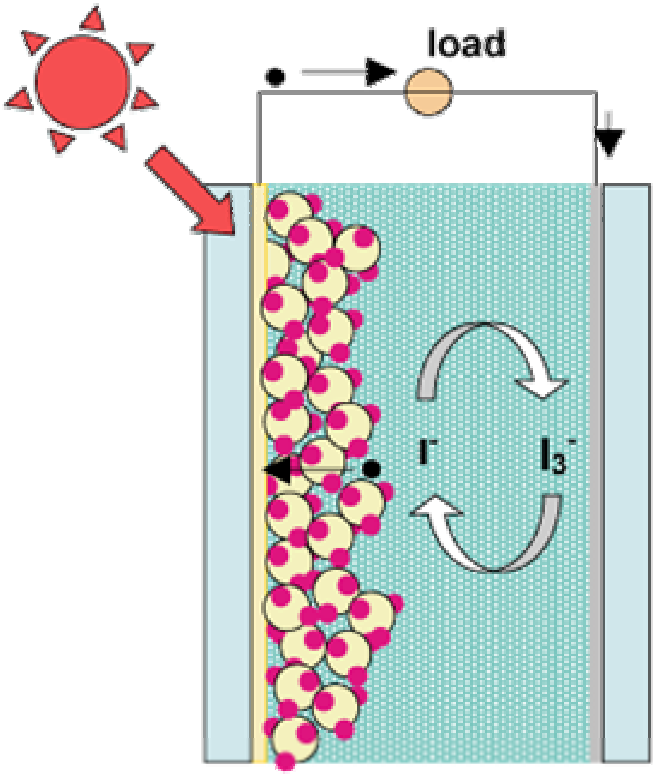

① Electrons of dye are exited by solar energy adsorption

② Electrons transfer from dye to FTO via TiO_2

③ Electrons get to counter electrode after working at external load

④ $1/2I_3^- + e^- \rightarrow 3/2\ I^-$ at counter electrode

⑤ $3/2\ I^- \rightarrow 1/2I_3^- + e^-$ at dye

TiO_2 electrolyte FTO/glass

Dye • electron Pt/glass(counter electrode)

Dye-Sensitized Solar Cells

- **Absorption occurs in dye molecules adsorbed at a highly porous structure of nanoparticles of transparent TiO_2**
  - Dye excited by incident photon of light
  - Dye excitation followed by electron injection into TiO_2 (n-type)
  - Electrons are transported to the front contact
    - Transparent conductive oxide layer (TCO)
  - Positive charge transferred from dye to a redox mediator ("interception") and then to the counter electrode
  - Dye recharged via redox electrolyte
  - Contact of redox electrolyte made by a catalyst-coated back contact
  - Mediator is returned to its reduced state and the circuit is closed

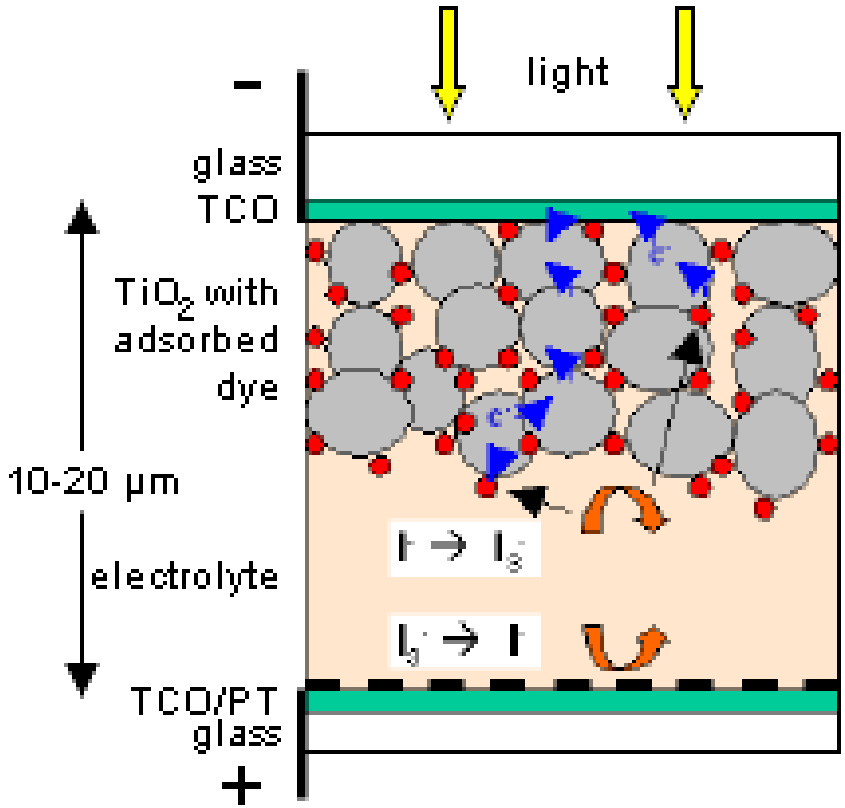

Fig. 1: Schema of dye-sensitezed solar cell

Kron, *et al.* (2003)

- **Working principles of the original electrolyte DSC**
  - Basic action relies on photoexcitation of the dye
  - Subsequent injection of the excited electron in the TiO_2
  - Regeneration of the dye via the I^- / I_3^- redox couple
- **Idealize TiO_2 network as columns with a diameter of 10-15 nm placed on the SnO_2/F (as in the electrolyte in DSC)**
  - Columns are immersed into the electrolvte

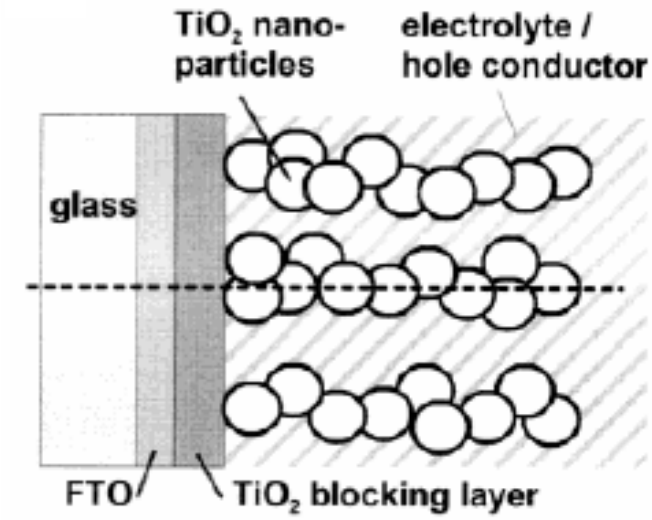

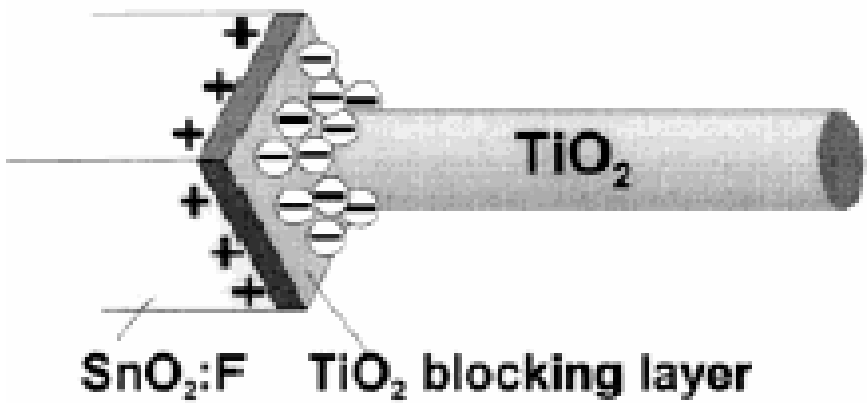

Kron, *et al.* (2003)

- **Because the TiO_2 is only moderately doped**
  - Charge within individual TiO_2 is too small to provide a band bending across the grain in excess of a few meV
  - Even this small charge in the colloids is screened by the Helmholtz layer of the electrolyte
    - Along the TiO_2 columns, there is no considerable electrical field

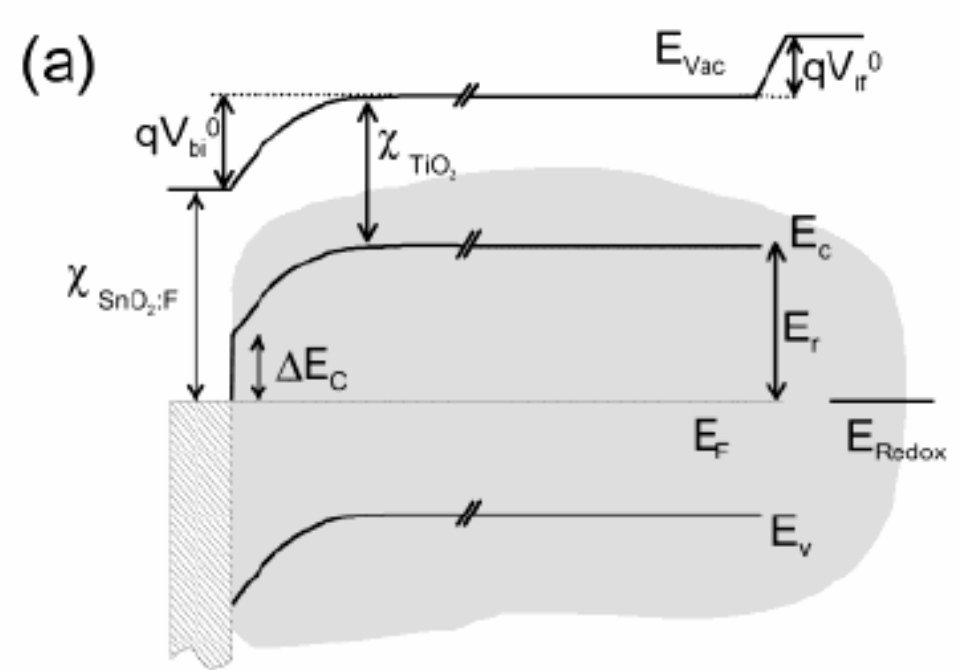

Left: Resulting band diagram for the conduction and valence band energies, E_c and E_v, in the center of a TiO_2 column immersed in the electrolyte

Kron, *et al.* (2003)

- **Position of the equilibrium Fermi level at the TiO_2 interface determined by the Fermi level of the electrolyte**
  - Interface dipole exists at the TiO_2 interface as indicated in the vacuum level, E_{vac}
    - Resulting from the polarity of the absorbed dye from the Helmholtz layer of the electrolyte
    - From the absorption of the Li+ cations which come closer to the interface than the I- anions

- **Arrangement of charged species close to TiO_2 interface**
  - Provides potential drop V_{if} that shifts the conduction band energy of the TiO2 downward with respect to E_{redox} of the electrolyte

- **Absence of electric field in major part of the TiO_2 network, transport of electrons toward the from electrode occurs by diffusion**

Regan and Gratzel (1991)

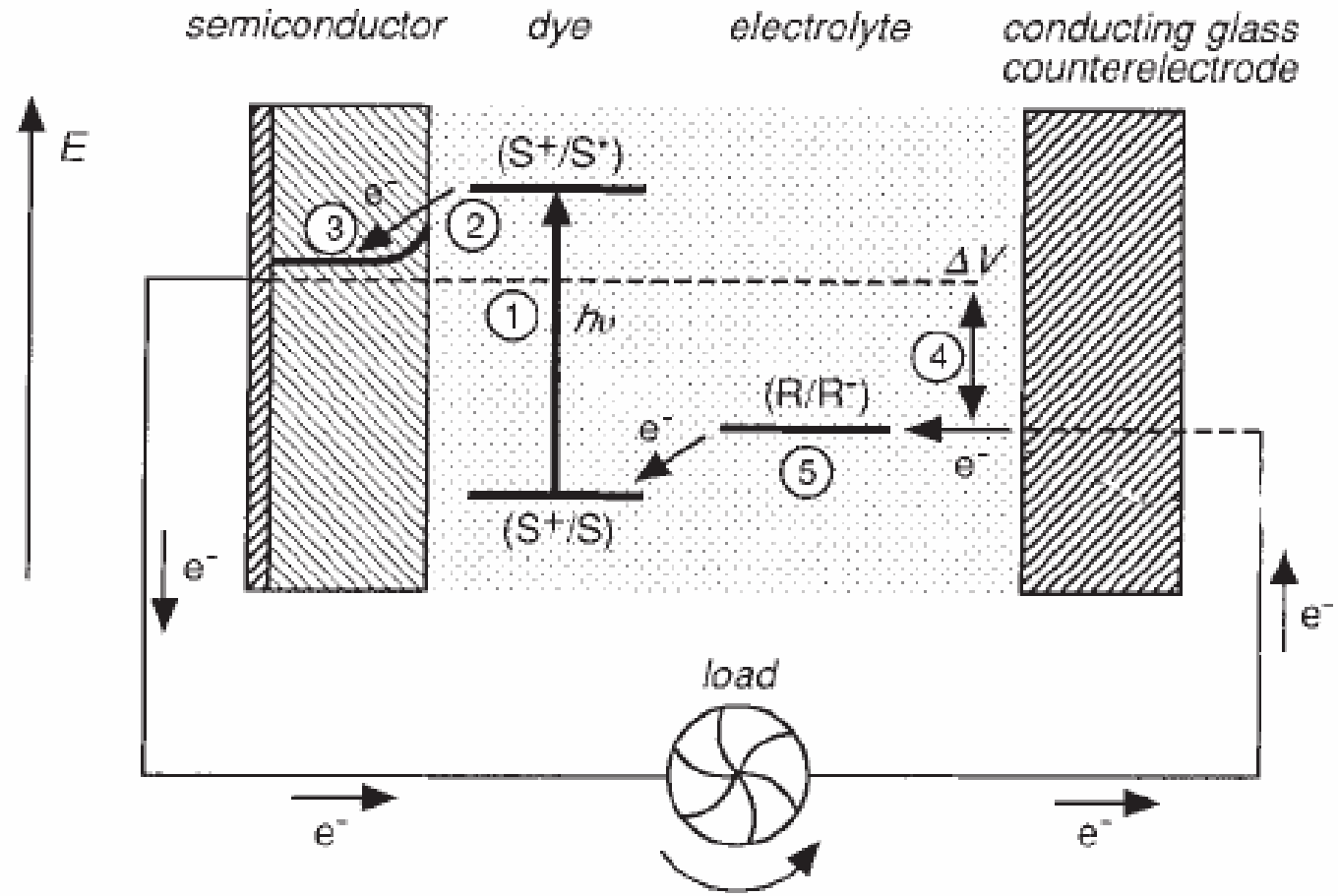

- Photovoltage ΔV generated by the cell corresponds to the difference between the Fermi level in the semiconductor under illumination and the Nernst potential of the redox couple in the electrolyte

Electron Transport in Nanoparticle Film

- **Electron transport determined by trapping and release of carriers from defect states at the surface or bulk of TiO_2**
  - Due to low values of the diffusion coefficient < 10^{-4} cm^2 s^{-1}
  - Not all of the injected electrons reach the back contact
    - Some may react instead with I_3^-, reducing the incident photo-to-current conversion efficiency (IPCE)

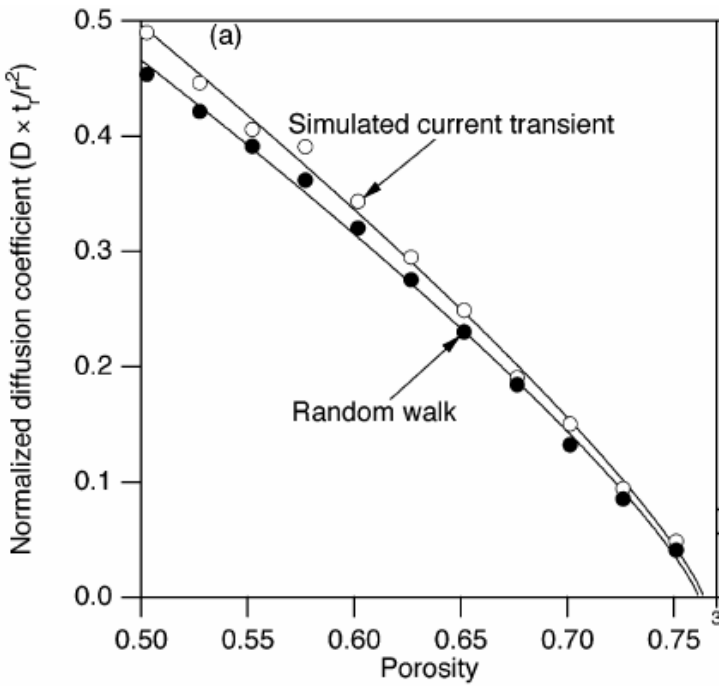

Regan and Gratzel (1991)

- **Problem**
  - Efficiency of such devices extremely low
  - Problem is of poor light harvesting
    - On smooth surface, monomolecular layer of sensitizer absorbs less than 1% of incident monochromatic light
    - Attempts to harvest light with multilayers of dye have been unsuccessful
  - Instability of dye another source of severe practical drawback

- **Solution**
  - Remaining option is to increase the roughness of the semiconductor surface
    - Increasing surface area
    - Can simultaneously be in direct contact with the redox electrolyte
  - Using nanometer size TiO_2 particles and new charge-transfer dyes, improve efficiency and stability of the solar cell

Regan and Gratzel (1991)

- **High surface area TiO_2 films deposited on a conducting glass sheet from colloidal solutions**
  - TEM image show colloids
  - Size of the particles and pores controlled by the size of particles in the colloidal solution
    - Parameters optimized to obtain efficient light harvesting while maintaining a pore size large enough to allow the redox electrolyte to diffuse easily

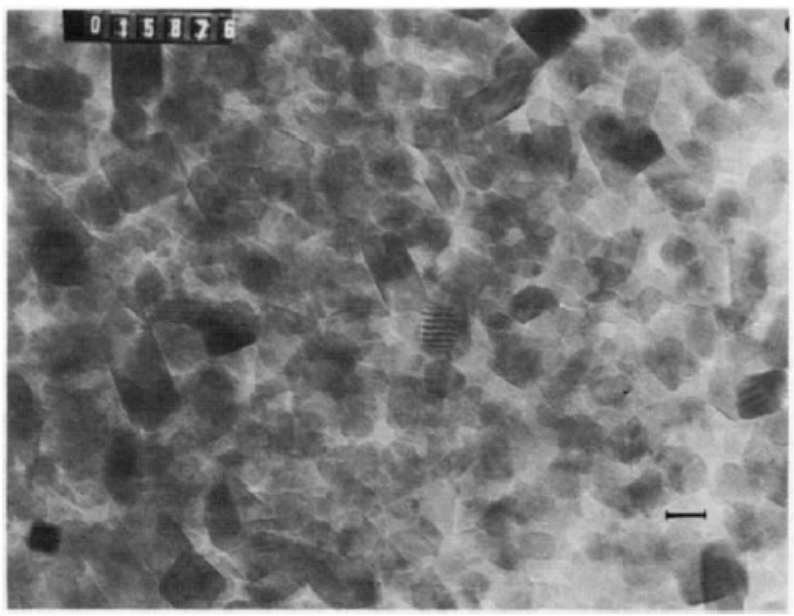

Scale bar represents 10 nm

Regan and Gratzel (1991)

- **Results of new dye**
  - Deposited monolayer of trimeric ruthenium complex, $RuL_2(\mu\text{-}(CN)Ru(CN)L_2')_2$

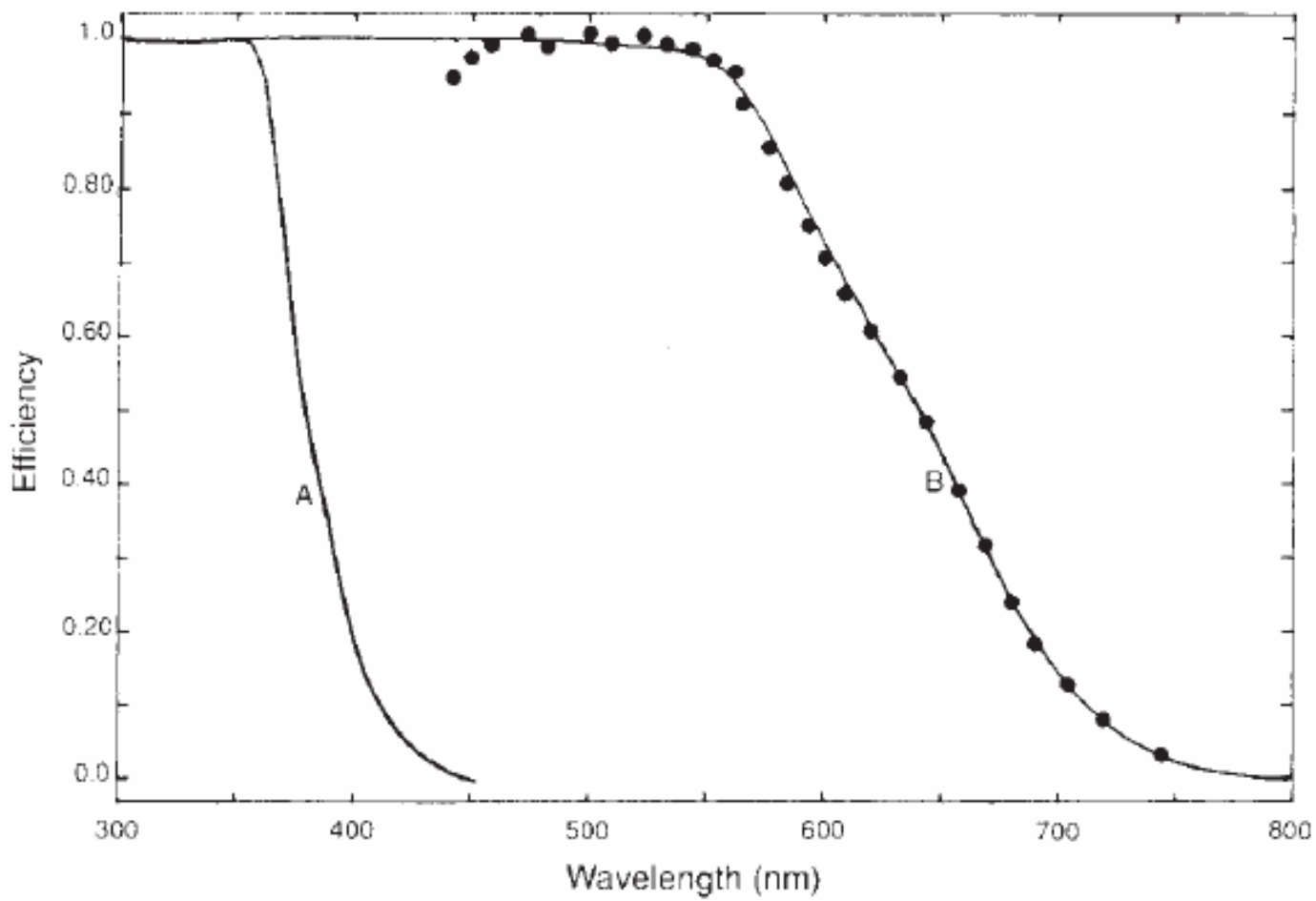

Improvements

- **Increase electron diffusion length in the anode by replacing nanoparticle film with array of oriented single-crystalline nanowires**

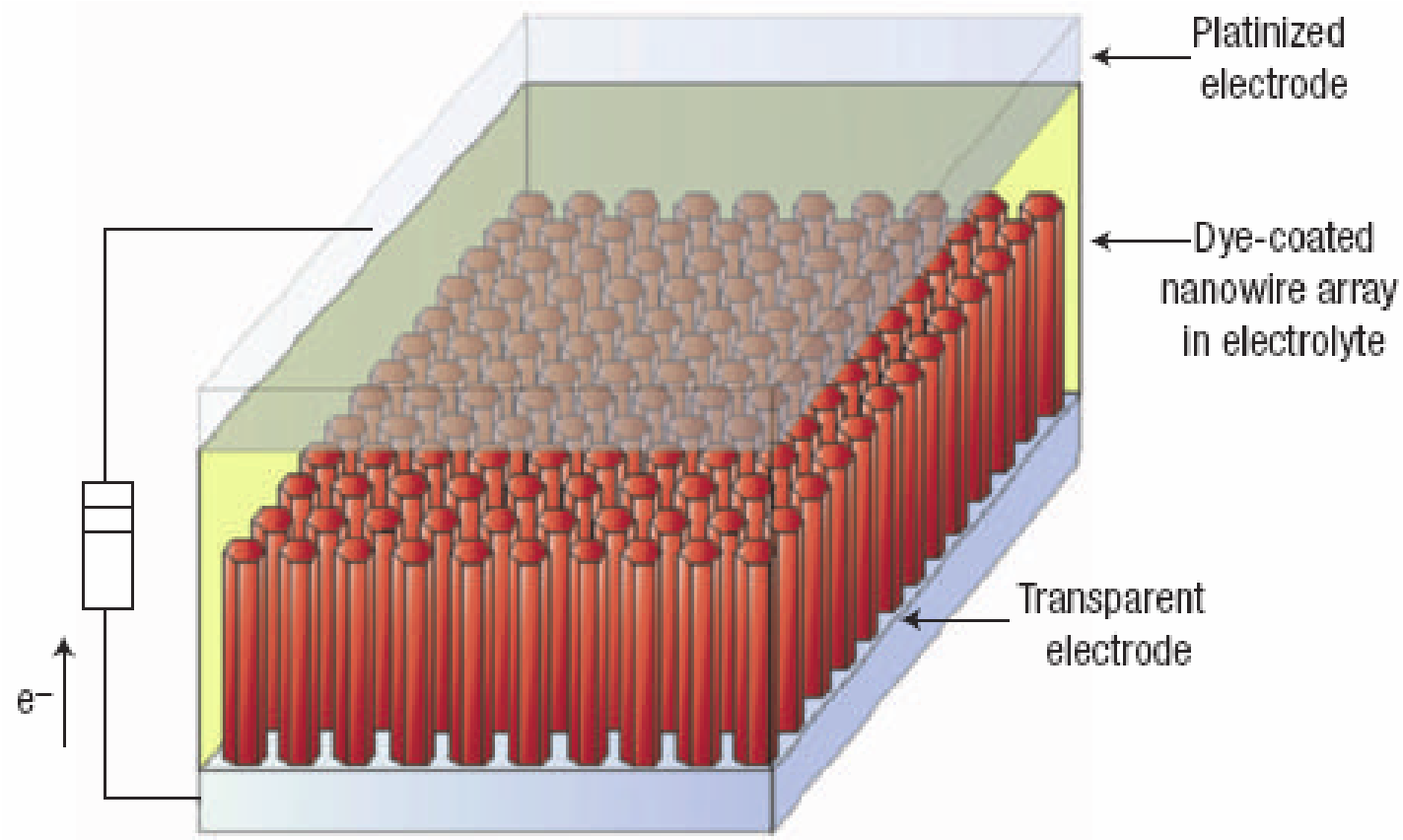

Left: Schematic diagram of the cell; light incident through the bottom electrode

Fabrication of Nanowire

- **ZnO nanowire arrays of high surface area in aqueous solution fabricated with seeded growth process**
  - Preparation of ZnO nanocrystals
    - NaOH solution in methanol (0.03 M) added to solution of zinc acetate dihydrate (0.01 M) in methanol at 60 C and stirred for 2 hours
    - Resulting nanoparticles spherical and stable in solution
  - Simple two-step process
    - ZnO nanocrystals (5 – 10 nm diameter) spin-cast several times onto a 4-inch Si (100) wafer
      - 50 – 200 nm thick film of crystal seeds
      - Wafer annealed at 150 C to ensure particle adhesion
    - Hydrothermal ZnO growth carried out by suspending wafer upside-down in open crystallizing dish
      - Aqueous solution of zinc nitrate hydrate and methanamine
      - Reaction time between 0.5 to 6.0 hours

Greene, *et al.* (2003)

- **SEM image show entire wafer coated with highly uniform, dense packed ZnO nanowires**

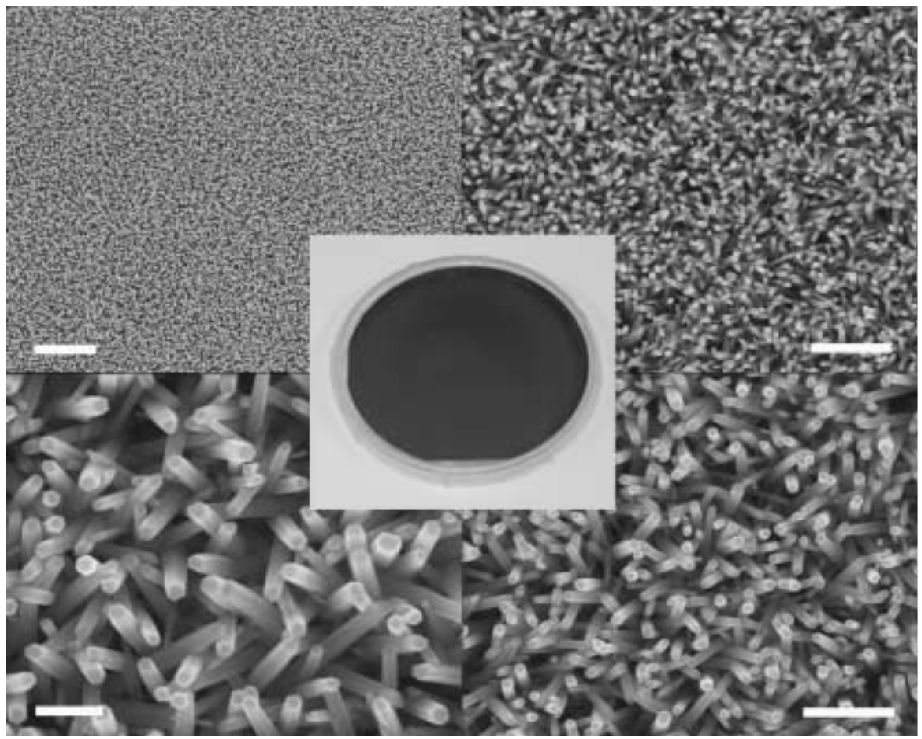

- **Typical synthesis 1.5 hours**
  - Diameter: 40 – 80 nm
  - Length: 1.5 – 2 μm
  - Arrays have surface area ~ 50 cm^2 per cm^2 of substrate

- **Longer reaction times**
  - Generate nanowires up to 200 to 300 nm wide and 3 μm long for a 6.0-hour reaction time

Modified Fabrication Process

- **Two-step process modified to yield long nanowires**
  - 10 – 15 nm thick film of ZnO quantam dots deposited on F:SnO_2 conductive glass (FTO) by dip coating
- **Boost aspect ratio by > 125 using polyethylenimine (PEI)**

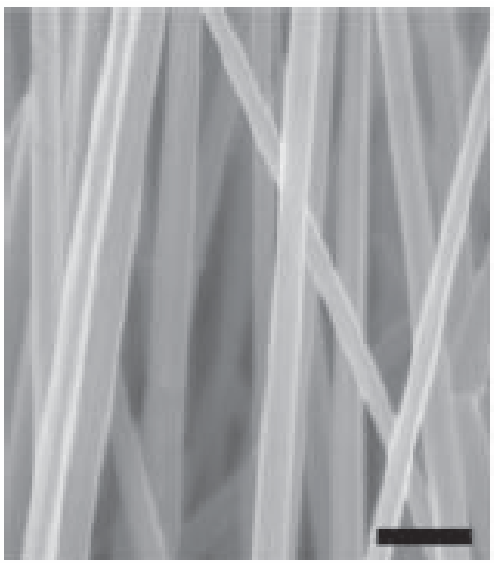

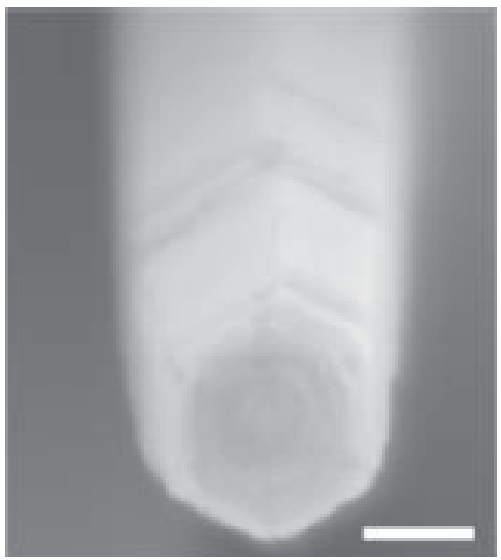

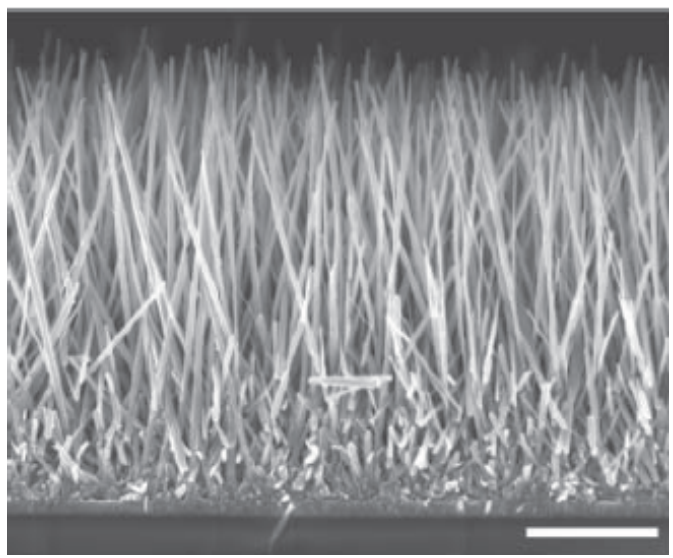

Evaluating PEI for Nanowire Growth

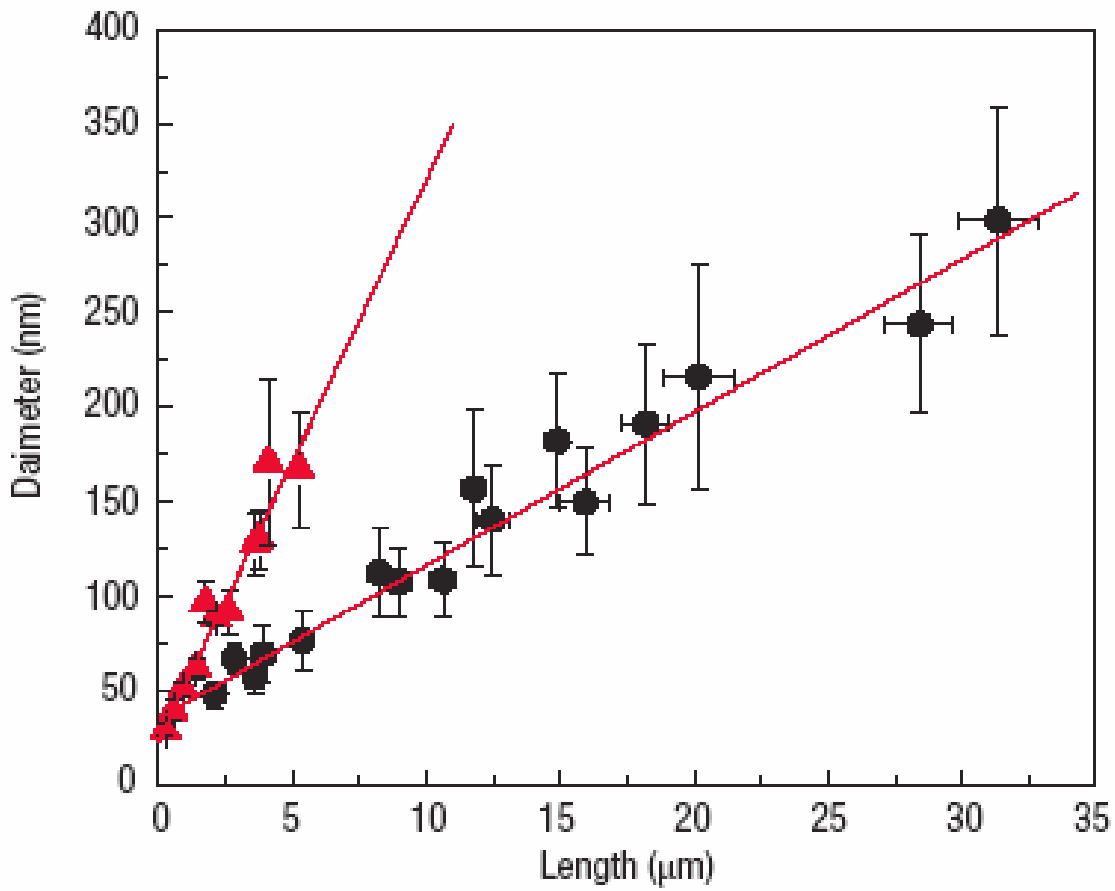

- **Plotting nanowire length against diameter at different growth times**
  - Red triangle: Without PEI
  - Black circle: With PEI

Wire Films

- **Wire films good electrical conductors along direction of wire axes**
  - 2-Point electrical measurements of dry arrays on FTO substrates gave linear current-voltage (I-V) traces
    - Indicate barrier-free contacts between nanowire and substrate
- **Individual nanowires extracted from arrays, fashioned into FETs using standard electron-beam lithography**
  - Determine resistivity, carrier concentration, and mobility
    - Resistivity: 0.3 to 2.0 Ω cm
    - Electron concentration: 1 – 5 x 10^{18} cm^{-3}
    - Mobility: 1 – 5 cm^2 V^{-1} s^{-1}
- **Estimate electron diffusivity using Einstein relation**

$$D = \frac{k_B T \mu}{e}$$

  - Electron diffusivity, D_n = 0.05 – 0.5 cm^2 s^{-1} for single dry nanowires
    - Several hundred times larger than the highest reported diffusivity for TiO_2 or ZnO nanoparticle films in operating cells
  - Conductivity of wire arrays increased by 5 – 20% when bathed in standard DSC electrolyte

VALIDATION

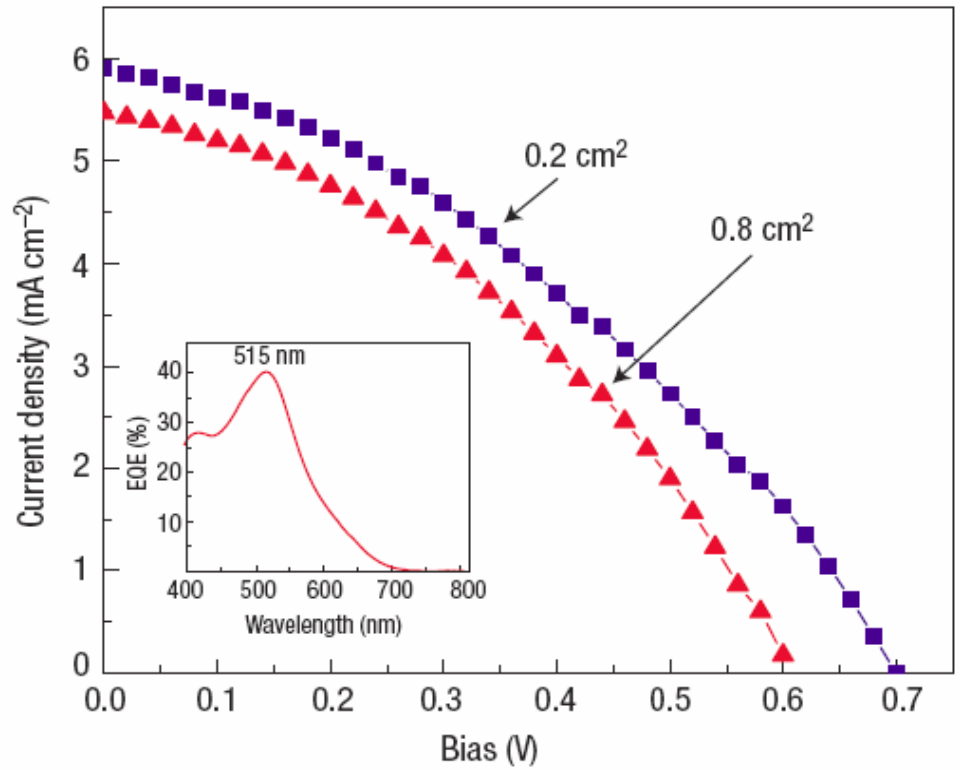

Top: Traces of current density against voltage (J-V) for two cells with roughness factors of ~ 200; small cell shows a higher V_{oc} and J_{sc} than the large cell

- **Solar cells constructed with wire arrays of various surface areas and tested in simulated sunlight**
  - Full sun intensity: 100 ± 3 mW cm^{-2}
  - Highest surface area device characterized by:
    - J_{sc} = 5.3 – 5.85 mA cm^{-2}
    - V_{oc} = 0.61 – 0.71 V
    - FF = 0.36 – 0.38
    - Efficiency η = 1.2 – 1.5%
- **External quantum efficiency of these cells peak at 40 – 43% near the absorption maximum of the dye**
  - Limited by relatively low dye loadings of the nanowire thin film

Effects of Light Intensity

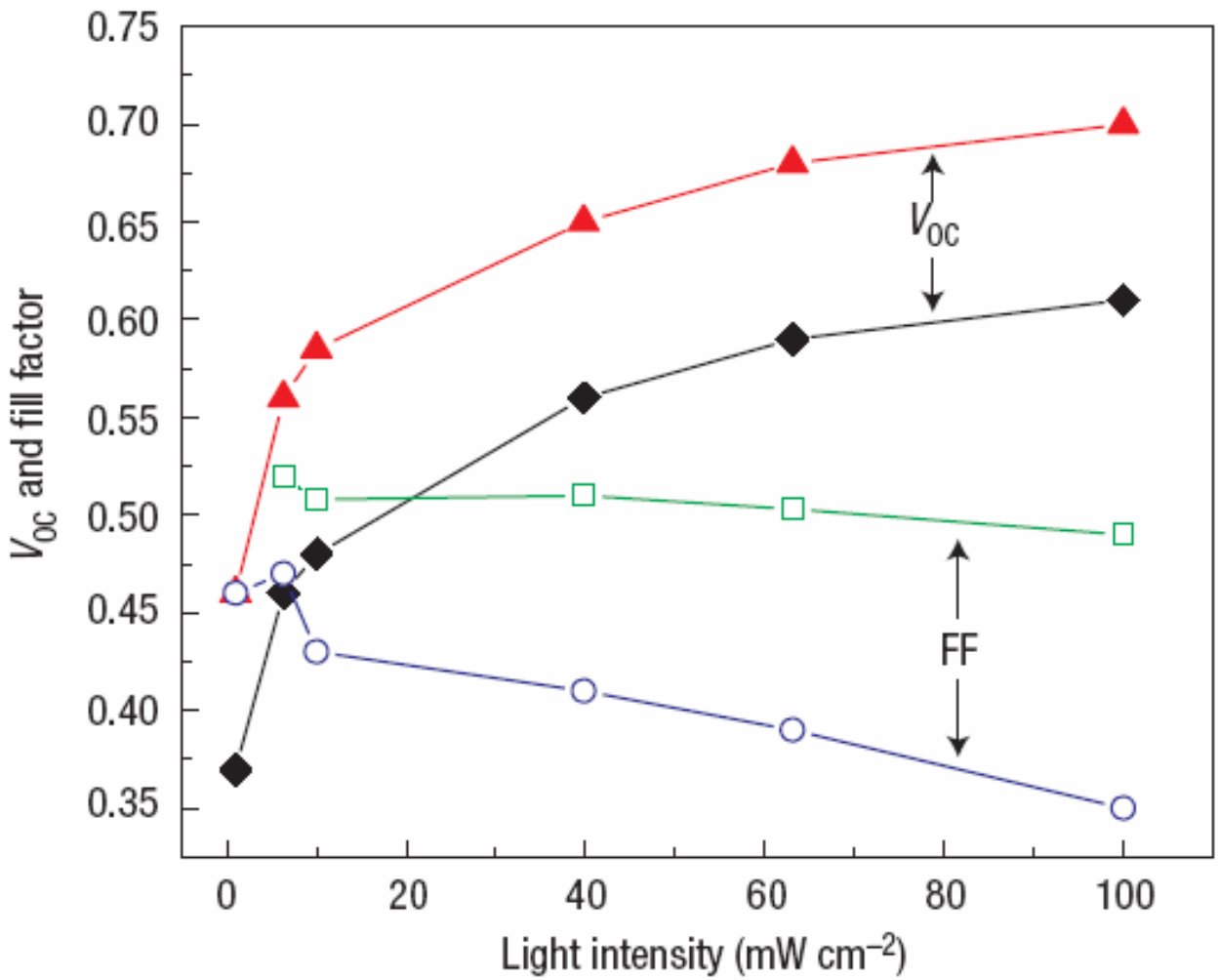

Top: Shows open-circuit voltage and fill factor against light intensity

Effects of Light Intensity

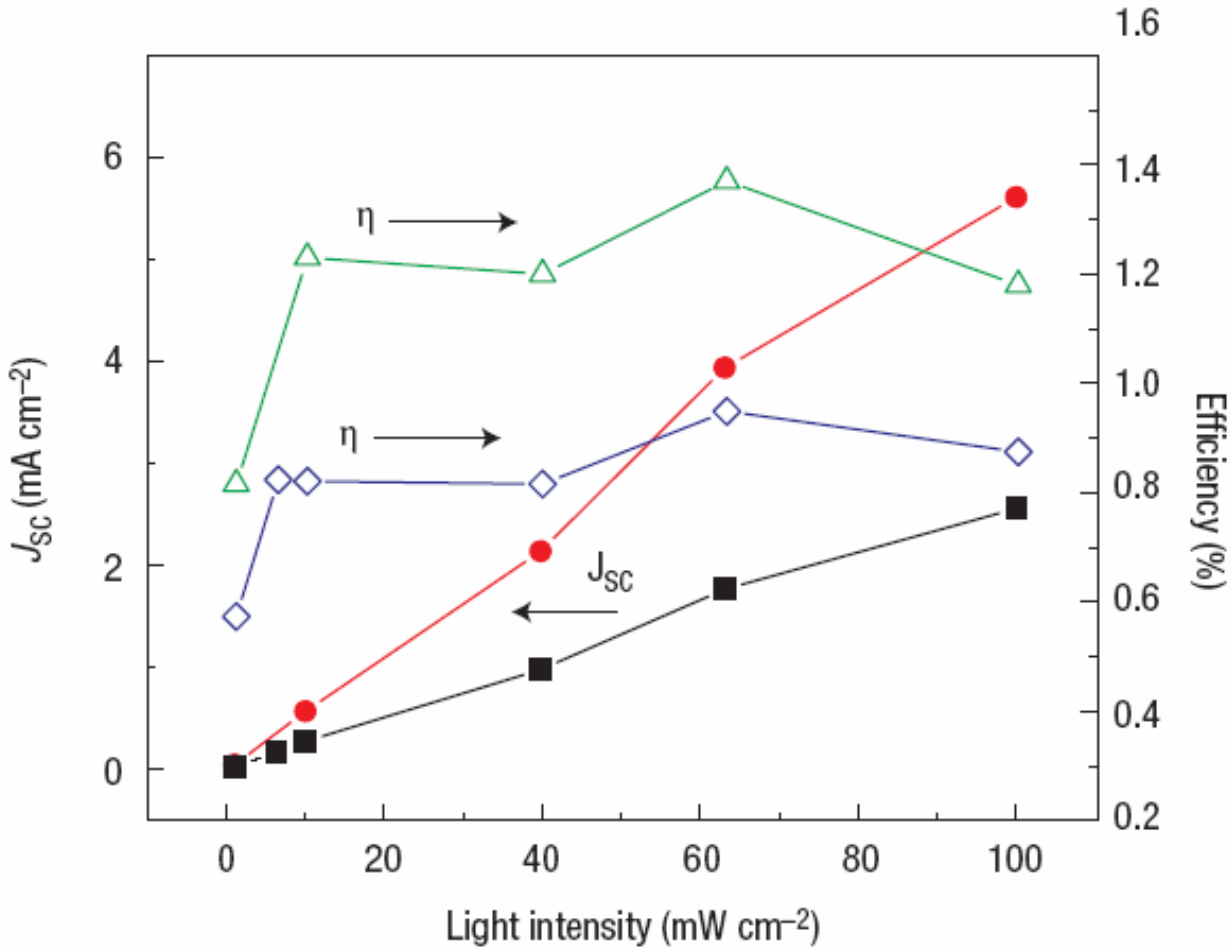

Top: Short-circuit current density and efficiency against light intensity for cells with roughness factors from 75 to 200.

Effects of Light Intensity

- **The open-circuit voltage and short-circuit current depend logarithmically and linearly on light flux, respectively**

- **Compared with nanoparticle cells**
  - Fill factors are low
  - Do not vary with cell size
  - Fall off with increasing light intensity owing to the development of a large photo-shunt of unknown origin

- **In general, cells of high roughness factor have low V_{oc} and fill factor, but high J_{sc} and efficiency**

Shortcomings

- **Insight into factors that limit DSC performance gained by comparing theoretical cell efficiencies with those of current cells**
  - Power conversion efficiency of a solar cell

$$\eta = \frac{FF \cdot \left| J_{sc} \right| \cdot V_{oc}}{P_{in}}$$

    - FF is the fill factor
    - J_{sc} is the current density at short circuit
    - V_{oc} is the photovoltage at open circuit
    - P_{in} is the incident light power density
- **Much of the shortfall due to poor absorption of low-energy photons by available dyes**
  - Efforts made to develop dyes and dye mixtures that absorb better at longer wavelengths
  - Thickening nanoparticle film to increase its optical density

Renouard, *et al.* (2002)

- **Optimal sensitizer for dye-sensitized solar cells should be panchromatic – absorbing visible light of all colors**
  - Ideally, all photons below a threshold wavelength of 920 nm should be harvested and converted to electric current
  - To absorb light below 920 nm, redox level (energy levels) of the sensitizers need to be tuned
    - Metal-to-ligand charge transfer transitions can be tuned to lower energy in 2 ways
      - Introduce ligand with a low lying π* molecular orbital
      - Destabilization of the metal t_{2g} orbital with a strong donor ligand
    - Heteroleptic complexes containing bidentate ligands with low lying π* orbitals together with others having strong σ-donating properties show impressive absorption properties
  - Geometrical isomerization (*cis-to-trans*) is another approach for tuning the spectral properties of metal complexes

Renouard, *et al.* (2002)

- **Synthesized functionalized hybrid tetradentate ligands and their ruthenium complexes**
  - Expected to show thermal stability and photostability
  - Donor units of the tetradentate ligand tune metal t_{2g} orbital energies
  - Acceptor units tune π* molecular orbitals
  - Axial coordination sites further used to fine-tune spectral and redox properties and to stabilize the hole that is being generated on the metal

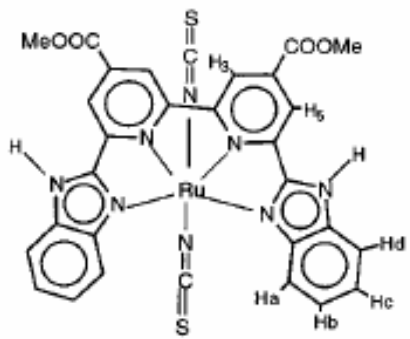

trans-[RuL^1(Cl)$_2$] 5

trans-[RuL^1(NCS)$_2$] 6

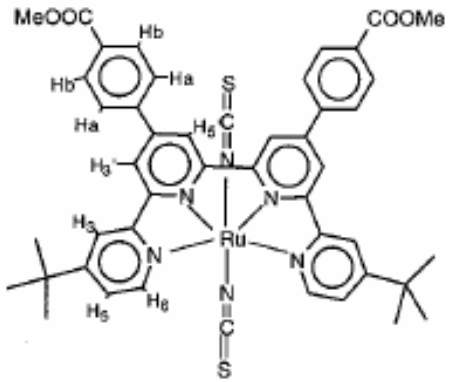

[RuL^2(Cl)$_2$] 7

[RuL^2(NCS)$_2$] 8

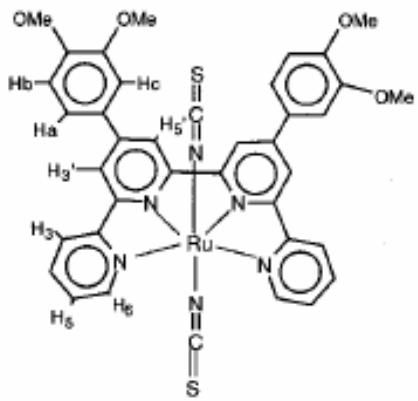

[RuL^3(Cl)$_2$] 9

[RuL^3(NCS)$_2$] 10

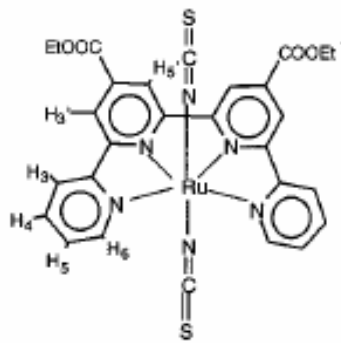

[RuL^4(Cl)$_2$] 11

[RuL^4(NCS)$_2$] 12

Comparing Performance

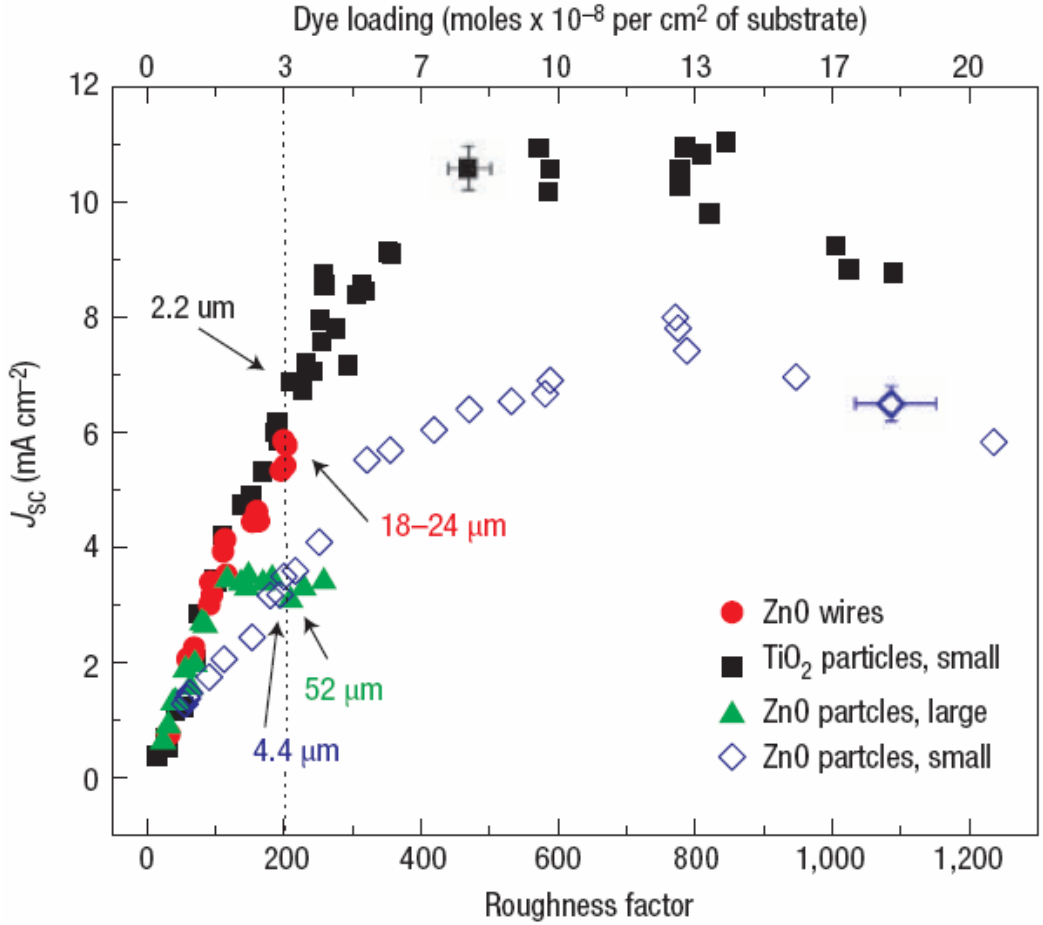

- TiO_2 films show a higher maximum current than either of the ZnO films and a larger initial slope than the small ZnO particles, consistent with better transport through TiO_2 particle networks

Comparing Performance

- **Hypothetical photoanode that maintained a near-unity carrier collection efficiency independent of roughness factor**
  - Trace out a line that gradually tapered off at high surface areas to a large J_{sc} value (> 25 mA cm^{-2})
- **Observe rapid saturation and subsequent decline of current from cells**
- **Nanowire cells generate considerably higher currents than ZnO particle cells**
- **Better electron transport**
  - Higher crystallinity

Nanoparticles vs. Nanowires

- **Switch from particle to wires affect kinetics of charge transfer**
  - Particle and wire films have dissimilar surfaces onto which the sensitizing dye absorbs
  - ZnO particles present an ensemble of surfaces having various bonding interactions with the dye
  - Wire arrays dominated by single crystal plane ({100})
    - Over 95% of total surface area

- **Dye-sensitized samples excited with 400-nm, 510-nm, and 570-nm pulses**
  - Free carrier concentration of the oxide was monitored with a mid-infrared probe
  - Transient responses for wires and particles considerably different

Nanoparticle vs. Nanowire

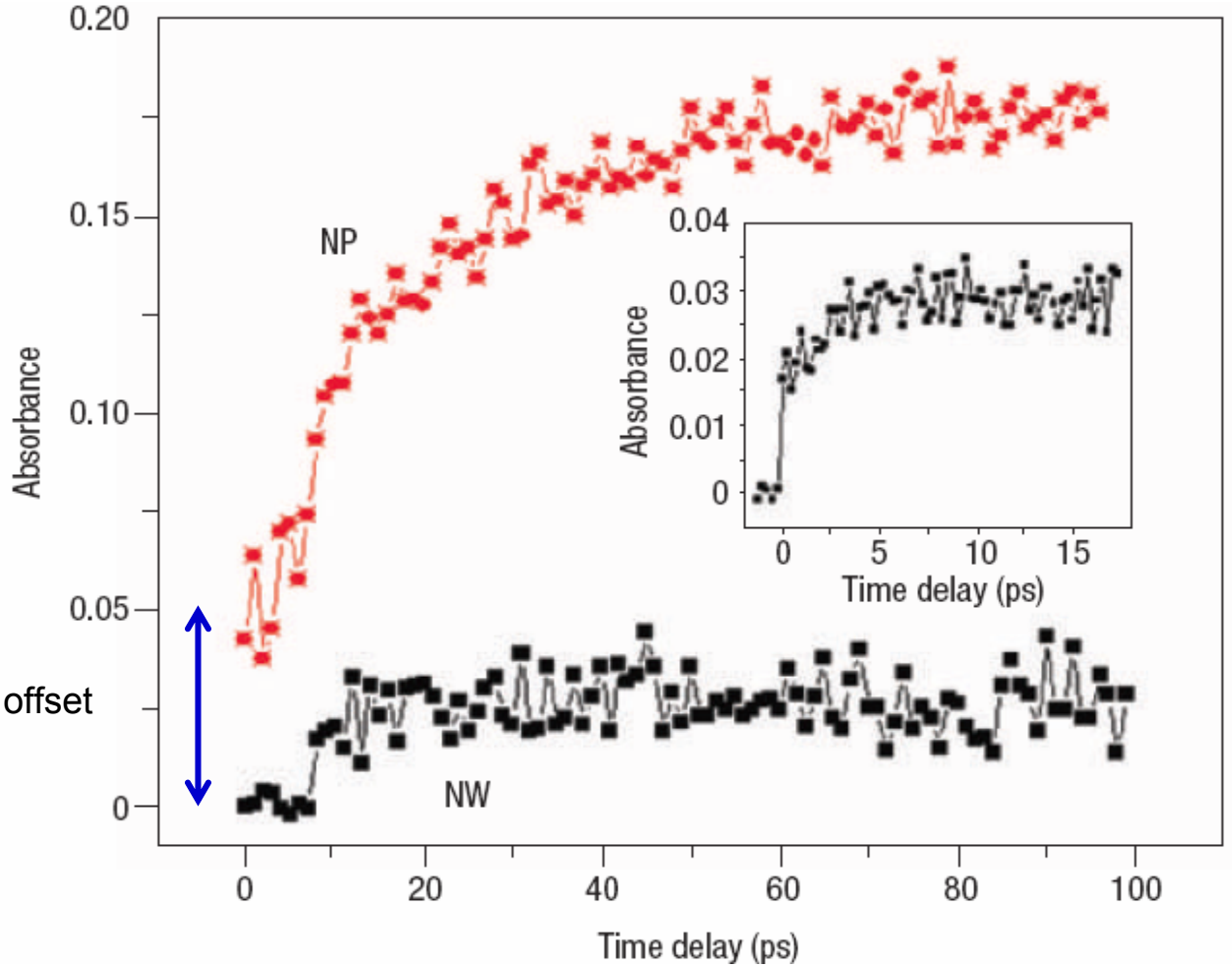

0.05 absorbance offset

- Transient mid-infrared absorption traces of dye-sensitized ZnO nanowire and ZnO nanoparticle films pumped at 400 nm

Conclusion

- **Nanowire dye-sensitized solar cell is an exciting variant of the most successful of the excitonic photovoltaic devices**
  - Wire arrays dominated by single crystal plane ({100}) that accounts for over 95% of their total area
  - Increases rate of electron transport
    - Time constants of 250 fs and around 3 ps
  - Nanowire electrode may be means to improving quantum efficiency of DSCs in the red region of the spectrum

- **Future Research**
  - Raising efficiency of nanowire cell depends on achieving higher dye loadings through an increase in surface area
  - Advantage of nanowire orientations useful for other types of excitonic photocells
    - *e.g.* Inorganic-polymer hybrid devices